Streamflow and hydrogen ion interrelationships identified using data-based mechanistic modelling of high frequency observations through contiguous storms

Timothy D. Jones and Nick A. Chappell

ABSTRACT

With the aim of quantifying the purely hydrological control on fast water quality dynamics, a modelling approach was used to identify the structure (and dynamic response characteristics or DRCs) of the relationship between rainfall and hydrogen ion (H^+) load, with reference to rainfall to streamflow response. Unlike most hydrochemistry studies, the method used makes no *a priori* assumptions about the complexity of the dynamics (e.g., number of flow-paths), but instead uses objective statistical methods to define these (together with uncertainty analysis). The robust models identified are based on continuous-time transfer functions and demonstrate high simulation efficiency with a constrained uncertainty allowing hydrological interpretation of dominant flow-paths and behaviour of H^+ load in four upland headwaters. Identified models demonstrated that the short-term dynamics in H^+ concentration were closely associated with the streamflow response, suggesting a dominant hydrological control. The second-order structure identified for the rainfall to streamflow response was also seen as the optimal model for rainfall to H^+ load, even given the very dynamic concentration response, possibly indicating the same two flow-paths being responsible for both integrated responses.

Key words | continuous-time transfer function, hydrogen ion, Llyn Brianne

Timothy D. Jones (corresponding author)
Nick A. Chappell
Lancaster Environment Centre,
Lancaster University,
Lancaster LA1 4YQ,
UK
E-mail: *t.jones1@lancaster.ac.uk*

INTRODUCTION

Short-term pulses of stream acidity can have a disproportionate negative effect on stream ecology (Lepori *et al.* 2003; Monteith *et al.* 2005), but models specifically of these short-term acid pulses in storms have received little attention since the early 1990s. Further, it is increasingly recognised that water quality sampling and/or *in situ* monitoring should be undertaken *continuously* at a high enough frequency to fully capture the dynamic behaviour of solute concentrations and load within streams (Kirchner & Neal 2013). Studies using continuous higher frequency sampling or *in situ* monitoring of a *wider range* of stream water quality variables are increasing (Table 1). However, even some of these studies may have insufficient sampling to capture the rapidly changing concentrations through storms within small headwater streams.

Several dynamic models capable of simulating changing stream acidity through storms were developed in the 1980s. These included the Birkenes model (Christophersen *et al.* 1982), MAGIC model (Cosby *et al.* 1985) and CAPTAIN model (Langan & Whitehead 1987). Significant differences in those catchment processes that are assumed to be the dominant controls of stream acidity exist between these models (Christophersen *et al.* 1990). The original MAGIC model of Cosby *et al.* (1985) assumed that the time series of stream H^+ concentration (with a weekly simulation time-step) is primarily a function of a time-varying geochemistry of a single soil unit combined with the effects of CO_2 de-gasing as soil-water exfiltrates into a stream. In contrast, the Birkenes model of Christophersen *et al.* (1982) assumed that stream acidity is also a function of the mixing of

doi: 10.2166/nh.2014.155

Table 1 | Examples of higher frequency continuous sampling and *in situ* monitoring intervals used in stream hydrochemistry studies, ordered by descending sampling frequency

Stream-water sampling frequency	Chemical determinands	Reference
10 min	TP	Jordan *et al.* (2007)
15 min	pH, conductivity	Robson & Neal (1990); Neal *et al.* (1992); Robson *et al.* (1993)
15 min	pH, conductivity	Hodgson & Evans (1997)
15 min	DO	Malcolm *et al.* (2006)
20 min	pH, conductivity	Bonjean *et al.* (2007)
1 hourly (approx.)	pH, Al species, TOC	Goenaga & Williams (1988)
1 hourly	TP	Bieroza & Heathwaite (2012)
6.5 hourly (average)	TP, SRP, TON, Si	Bowes *et al.* (2009)
7 hourly	pH, Al, Ca, Cl, conductivity, DOC, Fe, NO_3, Si, SO_4	Halliday *et al.* (2012)
7 hourly	pH, F, Br, I, Cl, SO_4, NO_2, NO_3, NH_4, TDN, DOC, K, Mg, Na, Ca, B, S, Si, Gran alkalinity, conductivity, Li, Be, Al, Sc, Ti, V, Cr, Mn, Fe, Co, Ni, Cu, Zn, As, Se, Rb, Sr, Mo, Cd, Sn, Sb, Cs, Ba, W, Pb, U, La, Ce, Pr	Neal *et al.* (2012); Kirchner & Neal (2013)
24 hourly (composite samples)	$^2H/^1H$ and $^{18}O/^{16}O$ isotopes	Birkel *et al.* (2010)

chemically distinct soil-waters sourced from two separate soil horizons, and the implicit effects of hydrological routing to and from these horizons. Other models assuming a key role of hydrological routing or pathways do, however differ in that they assume that fewer (i.e., one: Whitehead *et al.* 1988) or greater (i.e., three or more: Grip *et al.* 1985) numbers of water pathways are required to simulate the dynamics in stream acidity. Even after 20 years of further research into water pathways controlling stream chemistry, there is often no consensus as to the geochemical and hydrological structure of catchment models (e.g., whether they include one or more dominant strata-specific pathways or separate macropore flows) needed to simulate stream acidity or other water quality variables (Kirchner 2009). Advances in our understanding of uncertainty in hydrochemical modelling (e.g., Medici *et al.* 2012) do, however, provide ever greater evidence that with overly complex models many different combinations of processes (hydrological, geochemical or both) can simulate stream acidity. Consequently, accurate simulation of an output variable such as stream H^+ concentration does not necessarily mean that the dominant mechanism for the release of H^+ to streams has been represented accurately. Correct outputs may be simulated for the wrong reasons (Beven & Westerburg 2011). Models that have many more parameters than can be justified by the complexity of the dynamics of the variable to be simulated (i.e., overly complex models) are now seen as poor models because of the reduced identifiability (i.e., increased parameter uncertainty) arising from the routines used to identify optimal parameter sets. As a result of these two issues there is an increasing acknowledgement of the value of using parsimonious (i.e., efficient but simple) model structures (i.e., those that do not include too many hydrological or geochemical processes or pathways). Similarly, there is an awareness of the value of not fixing a model structure without first evaluating alternatives (e.g., not forcing the simulation of acid runoff to follow two water paths without also assessing the simulation capabilities of a single or numerous water pathways). This issue was appreciated following the early hydrochemical modelling work (e.g., Christophersen *et al.* 1993) but often ignored subsequently. The philosophy of the data-based mechanistic (DBM) modelling approach adheres to both of these principles (Young 2013). The first stage in the DBM approach is the application of a large number of mathematical relationships (often in the form of transfer functions), to describe the dynamics between observed input time series (e.g., rainfall, temperature), and output time series (e.g., H^+ concentration), and thereby form data-based models. Those identified models that do not meet strict mathematical-statistical

criteria are rejected. Finally, only those statistically valid models that also have a mechanistic (process) interpretation are accepted. This approach of not making *a priori* assumptions about the number of water pathways has been adopted in this study.

A major new water quality monitoring programme to help understand temporal and spatial change in stream biodiversity was initiated in 2012 and includes work on the Llyn Brianne Experimental Basins. These basins drain into the Llyn Brianne water supply reservoir (52°8′ 7″ N 3°44′ 50″ W) in the headwaters of the River Towy (Welsh: Afon Tywi) in upland Wales, United Kingdom. Water quality observations within these basins originally began in February 1981 with a view to better understand the effects of afforestation and liming on stream acidification (Stoner *et al.* 1984). The new water quality monitoring initiated in 2012 by Lancaster University and the Centre for Ecology and Hydrology forms a core part of an interdisciplinary project known as Diversity of Upland Rivers for Ecosystem Service Sustainability (DURESS) – see, e.g., http://www.lancaster.ac.uk/lec/sites/duress. This monitoring has involved systematic high-frequency measurement of variables that are known to affect and/or be affected by aquatic biodiversity, and include acidity, nitrate and carbon (see, e.g., Simon *et al.* 2009; Whitehead & Crossman 2012; Nelson *et al.* 2013). Variations in stream discharge characteristics are also known to impact aquatic biodiversity directly (e.g., Kennard *et al.* 2010) and indirectly through the regulation of nutrient load (Harmel *et al.* 2006), and so also form an integral part of the monitoring programme. Given the acknowledged speed of response of key water quality variables within these and other headwater streams (e.g., Kirchner *et al.* 2004), many of the water quality variables, notably pH, electrical conductivity (EC), nitrate, dissolved organic carbon (DOC), turbidity and temperature, have been monitored continuously *in situ* at 15-minute intervals. This continuous monitoring intensity for *this range* of water quality variables has not previously been achieved at Llyn Brianne or at any other site in the Cambrian Mountains (e.g., Plynlimon experimental basins: see, e.g., Kirchner & Neal 2013).

Interrelationships have been demonstrated between H^+ concentration and other water quality variables, notably macronutrients and metals (Grande *et al.* 2005; Evans *et al.* 2012), some of which have equal impacts upon aquatic biodiversity. Given the crucial role of H^+ concentration in understanding the dynamics of stream biogeochemistry, this first study utilising 15-minute sampled water quality data will focus on quantifying the temporal dynamics within H^+ concentration and load.

One of the most significant results of the aquatic biodiversity research in the Cambrian mountain region has been the detrimental impact of coniferous afforestation on systems formerly covered by upland grassland (e.g., Dunford *et al.* 2012). The enhanced scavenging of airborne sulphur and nitrogen compounds by forest canopies is one of the key reasons for this effect (Fowler *et al.* 1989). Recent reductions in the industrial emissions of these compounds has, however, led to local reductions in acid deposition (Langan *et al.* 2009) but with possible adverse impacts on leaching of DOC (Monteith *et al.* 2007). Given the local importance of land-cover to stream acidity, this study considers both conifer-affected and original moorland sites in parallel, and involves one replicate of each.

This new study focuses on modelling winter storm dynamics because this is the period when most dissolved hydrogen is exported from temperate catchments in northern latitudes (Fitzhugh *et al.* 1999; Halliday *et al.* 2012). Further work will address the changes in dynamics between winter and summer periods (cf. Yevenes & Mannaerts 2012). The DURESS field campaign began in late 2012, with December 2012 providing suitable rainfall and streamflow data for catchment modelling within the winter period, because of the numerous rainstorms that occurred over a short period (i.e., a time series with a high information content). The hydrogen ion measurements commenced in January 2013, but were affected by poorly quantified snowfall amounts, so that the first synchronous rainfall, streamflow and hydrogen data with similar environmental conditions to the December modelling period were available in February 2013.

Limited DBM modelling utilising high-frequency rainfall, discharge, and H^+ concentration data from Llyn Brianne has been undertaken by Littlewood (2003) and others. The dynamic interrelationships between these variables were identified using discrete-time (DT) transfer function routines within the previous versions of the CAPTAIN toolbox. The capability and reliability of these routines has been improved substantially over recent years

(Taylor *et al.* 2007). Within this study the latest routines for transfer function identification were used to explore similarly high-frequency dynamics. This study makes use of significant advances in the routines for continuous-time (CT) rather than DT models, which give more accurate models and parameter estimates where dynamics are very fast (Young & Garnier 2006; Young 2010; Littlewood & Croke 2013). The potential for greater reliability with these models is enhanced with the parallel advances in sensor technology, notably the digital differential pH sensors that have been developed over the last 20 years.

AIMS AND OBJECTIVES

Given the research sites, high-frequency observations and state-of-the-art modelling tools available, this study has aimed to develop fundamental understanding of the within-storm dynamics of H^+ concentration and load, in response to hydrological dynamics. This aim has been addressed with the following three objectives:

1. To identify the strength and characteristics of the hydrological control on H^+ response by identifying optimal dynamic relationships between rainfall and H^+ load (sampled at 15-minute intervals) and comparing with those between rainfall and streamflow response. Novel CT transfer function (CT-TF) routines are used to give more reliable relationships than the DT models used in previous water quality studies.
2. To further quantify the hydrological control on H^+ response by examining the streamflow to H^+ concentration relationships. In comparison to models forced by rainfall, these dynamic relationships were expected to be more easily identified given that both variables are measured on the same stream and streamflow is an integral of the resultant pathways of rainfall.
3. To interpret the identified models in terms of similarities and differences in the controls on short-term H^+ dynamics between upland grassland streams and those affected by conifer forestry (i.e., the dominant land-uses in upland Wales). This understanding is sought from quantification of the dynamic response characteristics rather than from the transport/mixing characteristics (cf. Weiler *et al.* 2003) examined by many other modelling studies (e.g., Ocampo *et al.* 2006; Ockenden *et al.* 2013).

DESCRIPTION OF REPLICATED, PAIRED CATCHMENTS

The experimental basins studied (Figure 1) are located in the uplands of mid-Wales (215–410 m above sea level), and all drain into the Llyn Brianne regulating reservoir. For reasons of consistency, existing catchment nomenclature (e.g., Robson & Neal 1990) was adopted here. Two streams were selected with rough, sheep-grazed grassland (LI6 and LI7), where *Molina* spp., *Juncus* spp. and *Festuca* spp. dominate (Reynolds & Norris 1990). Two further catchments (LI3 and LI8) contain planted stands of Sitka spruce (*Picea sitchensis* [Bong.] Carr.), Lodgepole pine (*Pinus contorta* Doug.) and/or Japanese larch (*Larix kaempferi* [Lamb.] Carr.). Hence, the study uses replicated, paired conifer and grassland catchments. The chosen micro-basins contain stream channels that attain second- or third-order upstream of the pH monitoring station, and the key basin characteristics are given in Table 2.

There is a maritime temperate climate at Llyn Brianne with a mean annual precipitation measured over an eight-year period in LI8 of 2,100 mm (Vanguelova *et al.* 2010). The bedrock beneath all of the catchments comprises shales, mudstones, greywackes and grits of the Lower Palaeozoic era (BGS 2005). A significant depth of glacial till is mapped above the solid geology on the lower slopes of LI6, LI7 and LI8 (BGS 2005). This is modified by solifluction and nivation processes on the intermediate slopes, with the headwaters of LI6 being mapped as a nivation hollow (Potts 1971). Podzol, Gleysol and Histosol soil units (following FAO-Unesco 1990) are present within the four study basins (Table 3). The headwaters of LI6, LI7 and LI8 are primarily covered by Histosols (Reynolds & Norris 1990). In contrast, Reynolds & Norris (1990) indicate that LI3 lacks soils with an organic stratum >0.40 m deep (criteria for Histosol classification), and instead has extensive Gleysol coverage (Table 3).

Between 1957 and 1959, LI3 was almost completely afforested with a combination of Sitka spruce (occupying 53% of maximum forest cover), Lodgepole pine (16%), Japanese larch (13%) and a Lodgepole pine/Japanese larch mix

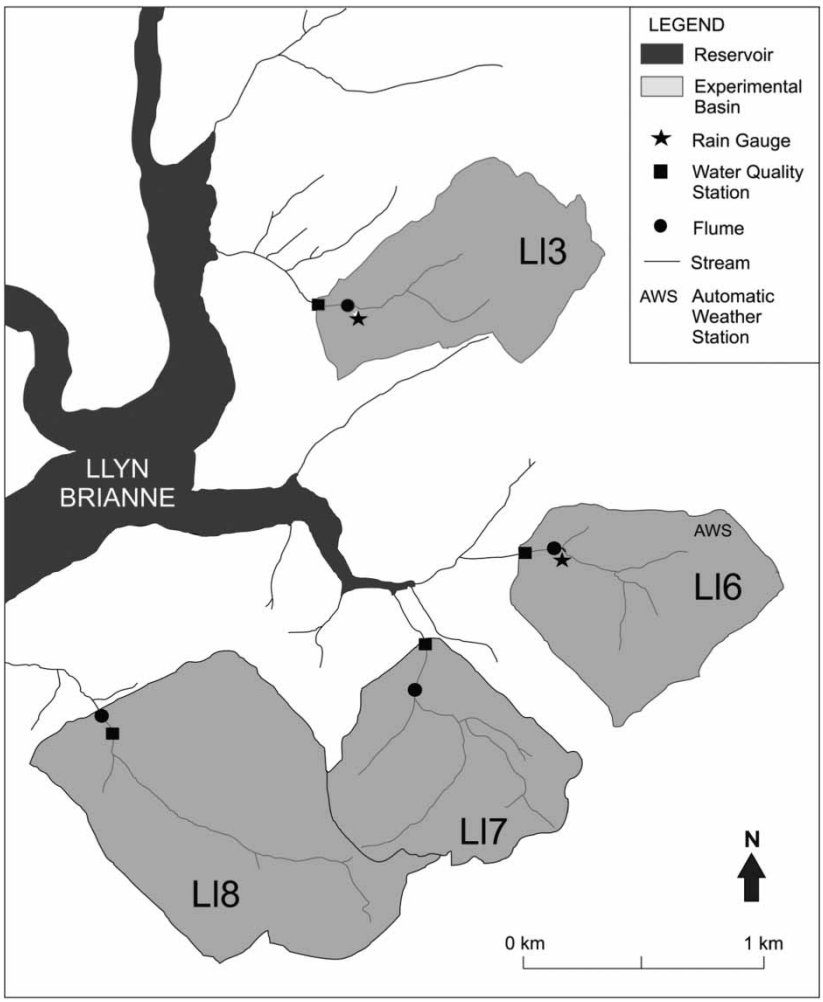

Figure 1 | Location of the LI3, LI6, LI7 and LI8 experimental basins in the vicinity of Llyn Brianne reservoir in mid-Wales, United Kingdom and the location of the instruments within these basins.

Table 2 | Characteristics of the LI3, LI6, LI7 and LI8 catchments at Llyn Brianne

Basin	Stream	Land cover	Area[a] (km^2)	Basin[b] slope ($m\ m^{-1}$)	Drainage density[c] ($km\ km^{-2}$)	Total hardness[b] ($mg\ CaCO_3\ litre^{-1}$)
LI3	Nant y Craflwyn	Coniferous plantation	0.81	0.107	2.08	8.3
LI6	Nant Esgair Garn	Grassland	0.69	0.122	2.84	12.9
LI7	Nant Rhesfa	Grassland	0.69	0.221	–	18.8
LI8	Trawsnant	Coniferous plantation	1.21	0.109	1.71	6.4

[a]Three-dimensional basin area upstream of the pH sensor derived using ArcGIS.
[b]From Weatherley & Ormerod (1987).
[c]From Littlewood (1989).

Table 3 | Proportion of the LI3, LI6, LI7 and LI8 basins at Llyn Brianne covered by each FAO-Unesco (1990) soil unit; adapted from Reynolds & Norris (1990)

Soil type	LI3	LI6	LI7	LI8
Podzols	0.47	0.45	0.33	0.44
Gleysols	0.48	0.15	0.18	0.09
Histosols	0.05	0.40	0.49	0.48

(15%). The forest within LI3 is part of the 13,500 ha managed Tywi Forest. The LI8 basin was afforested with Japanese larch (13%) in 1959, then in 1971 and 1977 with Sitka spruce (88% of forest cover: Reynolds & Norris 1990), and forms part of the Trawsnant plantation.

In June 1982, 2% of the LI3 basin was cleared along the stream banks (Stoner *et al.* 1984). A further 70% of the basin was clear-felled (CF) in the years 1995, 1998, 1999 and 2011. Around two-thirds of this CF area was replanted in years 1998, 2001 and 2002 (based on forest inventory maps provided by Natural Resources Wales). Within the headwaters of LI8 covered by Histosol soil, 4% of the forest was CF in 2012.

METHODOLOGY

Instrumentation, calibration and monitoring strategy

All four catchments were instrumented with identical stream equipment over the September 2012 to January 2013 period. Stream discharge was determined through measurement of water-level ('stage') at the point of critical flow in trapezoidal flumes. Flumes (constructed from fibreglass by Genesis Composites Ltd using the original mould of the Forth River Purification Board, Edinburgh) were cemented to the stream bed at locations so that they performed according to their published rating curve (FRPB 1986 Use of Glass Fibre Flumes. Fourth River Purification Board, Hydrology Department, unpublished report). The flume design was modified by this project by adding a tapping-point for stage measurement at the point of critical flow. The calibration was checked at each flume using salt-dilution gauging (Shaw *et al.* 2010). Water-level was measured using 0 to 2.500 m H_2O CTWM82X5G4C3SUN pressure transmitters (First Sensor AG, Puchheim) that were monitored every second and the data integrated and saved at 15-minute intervals using a CR1000 data-logger (Campbell Scientific Ltd, Shepshed).

Rainfall was measured in LI6 and LI3 (Figure 1) using tipping-bucket rain-gauges calibrated to record every 0.20 mm of rainfall (SBS500: Environmental Measurements Ltd, Newcastle).

Measurement of pH was undertaken using digital differential pH sensors (model: pHD-SC) combined with an SC200 controller (Hach Lange, Düsseldorf) and recorded at 15-minute intervals using further CR1000 data-loggers. The sensor was recalibrated at intervals determined by the sensor-controller system. *In situ* monitoring of other water quality variables (turbidity, nitrate, DOC, total organic carbon, colour and EC) was also undertaken at the locations of the pH sensors, but these data are not reported here.

All data were downloaded from the data-loggers on a weekly basis, and manual pH and water depth readings used to check for sensor malfunction; no such malfunctions were observed. Data were quality assured using dedicated Matlab programmes (Mathworks, Natlick) on a weekly basis, and erroneous numerical values (primarily associated with battery exchanges) replaced with Not-a-Number values.

From 1986 to 1989, the stream pH and stage had been monitored at a site 22 m upstream of the pH sensor in LI3 (Bird *et al.* 1990). During this earlier work, stage was measured using a pHOX 80PL system (pHOX Systems Ltd, Shefford). A stage–discharge relationship for the stage-board location was determined from extensive salt-dilution gauging (Littlewood 1989). The pH was measured using a Russell CE7NHL gel-filled combination electrode (see Thermo Fisher Scientific, Beverly) and pHOX 100 DPM sonde that was recorded every 15 min using a Technolog data-logger (Technolog Ltd, Wirksworth). Data from this earlier work were provided by the Environmental Information Data Centre of the Natural Environment Research Council (Licence: Llyn Brianne 22062012), and were used to help address Objectives 1 and 3 of this new study.

CT transfer function modelling using the DBM approach

The first stage of the DBM modelling process involved fitting a range of transfer function models to the data. For production of model parameter estimates in highly dynamic

systems, CT transfer functions (CT-TF) can be advantageous over DT transfer functions, as noted earlier. The former describe systems using differential equations and are more difficult to estimate than the latter, which are based on difference equations. A CT-TF for a purely linear single input, single output system can be given as follows:

$$\begin{cases} x(t) = \dfrac{B(s)}{A(s)}\, u\,(t - \tau) \\ y(t) = x\,(t) + \xi(t) \end{cases} \tag{1}$$

where $u(t)$ is the deterministic input signal, $x(t)$ is the noise-free output signal, $y(t)$ is the noisy output signal, $\xi(t)$ is the noise and τ is the pure time delay (i.e., delay between an input and the first response in an output) in units of time. $A(s)$ and $B(s)$ are polynomials in the derivative operator $s = \mathrm{d}/\mathrm{d}t$ as follows:

$$A(s) = s^n + a_1 s^{n-1} + \ldots + a_{n-1} s + a_n \tag{2}$$

$$B(s) = b_0 s^m + b_1 s^{m-1} + \ldots + b_{m-1} s + b_m \tag{3}$$

where n and m can be any positive integers with $m \leq n$. These equations are able to be expanded for multivariable systems, i.e., multiple input (e.g., rainfall and temperature) and single output (e.g., streamflow) or multiple output (e.g., streamflow and H^+).

When input, $u(t)$, and output, $x(t)$, observations have been made at a constant sampling interval, Ts (i.e., in discrete time), then the sampled signals are represented as $u(t_k)$ and $x(t_k)$ respectively, and the output observation equation is as follows:

$$u(t_k) = x(t_k) + \xi(t_k)\ k = 1, \ldots, N \tag{4}$$

where $x(t_k)$ is the sampled value of the noise-free unobserved output (x_t), which for data sampled in DT is assumed to be contaminated by noise, $\xi(t)$. The noise is independent of the input signal, $u(t_k)$, and represents the combination of distributed unmeasured inputs, modelling error and measurement error (Garnier *et al.* 2008).

The latest version of the RIVCBJID (*R*efined *I*nstrumental *V*ariable CT *B*ox-*J*enkins *ID*entification) algorithm was used here to identify a range of CT-TF model structures (Young 2008) using the CAPTAIN toolbox within the Matlab programming environment (Taylor *et al.* 2007). Within this routine, high-order noise is removed from the data (i.e., dynamics in the system that are much quicker than the quickest time constant) and which hinder identification of true model structure. The skill in the RIVCBJID routine also arises from its use of information within the covariance matrix (see Box *et al.* 2008).

Model structure is typically presented as a *triad* of denominator-numerator-delay within square parentheses, indicating the number of denominators (a terms in the lower part of the transfer function equation), the number of numerators (b terms in the upper part of the transfer function equation) and the number of pure time delays, τ (e.g., Chappell *et al.* 2012).

The identified models are assessed statistically using a measure of simulation efficiency ${R_t}^2$ and the Young Information Criterion (*YIC*). The ${R_t}^2$ is given as Equation (5)

$$R_t^2 = \frac{\sigma^2_{\text{error}}}{\sigma^2_{\text{obs}}} \tag{5}$$

where σ^2_{error} is the variance in the model residuals and σ^2_{obs} the variance in the observed data. This measure of simulation efficiency is equivalent to the simplified form of the Nash and Sutcliffe statistic and so differs from the R^2 that uses the variance in the model output as the denominator. The *YIC* is an objective statistical measure given as:

$$YIC = \log_e \frac{\sigma^2_{\text{error}}}{\sigma^2_{\text{obs}}} + \log_e\{\text{NEVN}\} \tag{6}$$

The first term within Equation (6) is a measure of the model efficiency (see Equation (5)) and the second term, normalised error variance norm, is a measure of the degree of over-parameterisation (Young 2001). Generally, as model complexity increases, so does the ability to capture more and more of the dynamics in the observed time series, but at the expense of increasing parametric uncertainty. There is, therefore, an optimum complexity (or 'model order') given that more complexity increases the uncertainty in the individual parameters identified. The *YIC* is a measure of whether the model has become overly complex (i.e., too many parameters) given the amount of information contained within the observed data series. A change of +1.0

or greater in *YIC* as model order is increased indicates that the model structure has become too complex for the information contained in the time series, i.e., over-parameterised (Ockenden & Chappell 2011), and the simpler model should be accepted as the optimal order.

The procedure for identifying the optimal model structure using these two measures begins by identifying the first-order model (from those convergent models) with the highest R_t^2 that does not have complex roots (see Box *et al.* 2008). Where second-order models have a higher R_t^2 than that of the optimal first-order model, these models are then examined for a change in the magnitude of the *YIC* from first to second-order models. If a second-order model: (i) has a higher R_t^2 than the optimal first-order model, (ii) its *YIC* is less than +1.0 different to the first-order model, (iii) it does not have complex roots, (iv) it does not exhibit oscillatory behaviour, and (v) the sign (±) of the two identified roots are the same, then this model is now accepted as the optimal structure. This procedure is repeated for third-order models, then fourth and so on. Models with a structure higher than sixth order are not normally examined because they are invariably over-parameterised. Typically, with rainfall to streamflow models attempts are made to identify models with between zero and six pure time delays. Consequently, by attempting to identify models from first-order to sixth-order with zero to six pure time delays, this gives 182 possible model structures to be identified using RIVCBJID. Many of these possible structures will not give convergent solutions.

Within this study, uncertainty in the model parameters was assessed using 1,000 Monte Carlo realisations of the optimal A and B terms (Equations (2) and (3)) combined with uncertainty information identified by the RIVCBJID routine. The second- and higher-order models were then decomposed into first-order components (with different structures) using partial fraction expansion (see Box *et al.* 2008). The resultant *a* and *b* terms were then presented as the dynamic response characteristics (DRCs) of the time constant (*TC*), steady state gain (*SSG*) and proportion of the response following a particular pathway (e.g., a fast response pathway, fast%):

$$TC = \frac{\Delta t}{a} \tag{7}$$

$$\mathrm{SSG} = \frac{b}{a} \tag{8}$$

$$\mathrm{fast}\% = 100\left(\frac{\mathrm{SSG}_2}{\mathrm{SSG}_1 + \mathrm{SSG}_2}\right) \tag{9}$$

where Δt is time-step of the observations (i.e., 15 min), SSG_1 is the SSG of the slow response pathway and SSG_2 is the SSG of the fast response pathway. The *TC* is the residence time of the response (i.e., not the residence time of a water particle or H^+ atom) between a rainfall input and either a streamflow or H^+ load output. Additionally, for a rainfall to streamflow model, the *TC* of a purely linear transfer function model is equal to the change in catchment moisture storage (mm/15 min) relative to the change in streamflow (mm/15 min). The SSG for a purely linear rainfall to streamflow model is the runoff coefficient between observed rainfall and the simulated streamflow. Lastly, further diagnostic tests (e.g., oscillatory behaviour in the impulse response function; presence of imaginary components in the derived *TC*s) were undertaken on the identified model structures and parameters as additional rejection criteria, prior to interpretation of the statistically acceptable models.

MODELLING RESULTS AND DISCUSSION

Rainfall to streamflow modelling and interpretation

Streamflow is the resultant integral of often complex pathways of response within a catchment. Identification of the most parsimonious set of DRCs that represent the principal mode(s) of rainfall–streamflow response may allow interpretation of the dominant water pathways of this response (Weiler *et al.* 2003; Chappell *et al.* 2006). Similarity between these purely hydrometric DRCs with those for response between rainfall and H^+ load may then indicate the role of water pathways in the propagation of component H^+ responses to streams (Part of Objective 1). To address the necessary initial hydrometric step, the RIVCBJID algorithm was applied to rainfall and streamflow data for a contiguous sequence of nine winter storms that were recorded between 19 December 2012 and 3 January 2013 within each catchment.

A range of purely linear models from first-order structures to sixth-order structures were identified, and each had a pure time delay between the onset of a rainfall event and a response in the stream of between zero and 90 minutes (i.e., six observation time-steps). The most efficient 20 models identified (ordered by R_t^2) for one of the four catchments (LI7) as an example, are shown in Table 4. The optimal models (i.e., high R_t^2, but without a $\geq +1.0$ change in *YIC* compared to lower order models) for all four catchments are shown in Table 5.

The use of purely linear CT-TFs has produced optimal models with at least 90% efficiency (R_t^2) of streamflow simulation (Table 5). Optimal models for all four basins had a [2 2 τ] structure, therefore all models simulated streamflow using only five parameters (i.e., two *a*-terms, two *b*-terms and a pure time delay) and so should be considered highly parsimonious relative to models (DBM, conceptual or physics-based) derived in many other studies (see Jakeman & Hornberger 1993; Young 2001; Beven 2012). The optimal model for LI7 and LI8 had a zero pure time delay ($\tau = 0$), while for LI3 and LI6 a pure time delay of one time step ($\tau = 1$) was identified and hence similar.

The rainfall–streamflow models for all four catchments (Figure 2) did not systematically under-predict (or over-predict) storm peaks, or systematically over-predict (or under-predict) lower flows. This provides an explanation as to why the range of non-linear transforms (following Young 2001) applied to input time series did not show any improvement in CT-TF simulation efficiency over the purely linear models and so are not presented here.

Within the DBM procedure, identified model structures are interpreted in terms of hydrological mechanisms. This initially involved decomposition by partial fraction expansion (see Box *et al.* 2008). For rainfall–streamflow systems,

Table 4 | The most efficient 20 rainfall–streamflow CT-TF models for the LI7 basin for the period 19 December 2012 to 3 January 2013, arranged according to their R_t^2

den	num	delay	*YIC*	R_t^2	*BIC*	S2 ×100	condP ×10
4	4	0	− 6.5635	0.9254	− 9,503.25	0.1040	9.254
2	3	0	− 4.6962	0.9208	− 9,442.03	0.1104	9.208
4	4	1	− 6.5819	0.9204	− 9,406.03	0.1109	9.204
2	***2***	***0***	***− 7.0686***	***0.9203***	***− 9,440.34***	***0.1111***	***9.203***
2	3	1	− 6.1001	0.9180	− 9,387.42	0.1142	9.180
2	2	1	− 7.0278	0.9143	− 9,332.25	0.1194	9.143
2	3	2	− 6.2497	0.9105	− 9,257.61	0.1247	9.105
4	4	2	− 5.8811	0.9051	− 9,154.84	0.1322	9.051
2	2	2	− 6.8518	0.9024	− 9,144.88	0.1359	9.024
2	3	3	− 6.0968	0.8976	− 9,063.30	0.1426	8.976
3	3	3	− 8.2699	0.8886	− 8,937.95	0.1553	8.886
2	2	3	− 6.6024	0.8858	− 8,917.80	0.1592	8.858
2	3	4	− 5.8462	0.8806	− 8,841.78	0.1664	8.806
2	2	4	− 6.3146	0.8649	− 8,677.15	0.1882	8.649
2	3	5	− 5.5455	0.8593	− 8,606.06	0.1961	8.593
4	4	5	− 5.5866	0.8515	− 8,509.64	0.2069	8.515
2	2	5	− 6.0174	0.8403	− 8,436.60	0.2226	8.402
3	4	6	− 2.2450	0.8389	− 8,395.57	0.2245	8.389
1	2	0	− 7.4547	0.8373	− 8,454.92	0.2266	8.373
1	2	1	− 7.8174	0.8356	− 8,432.72	0.2291	8.356

The term den is the number of transfer function denominators (recession or 'a' parameters), num are the number of transfer function numerators (gain or 'b' parameters), delay is the pure time delay between rainfall and runoff response, *YIC* is the Young Information Criterion and R_t^2 is the efficiency measure. Terms *BIC* (Bayesian Information Criterion), S2 and condP are additional measures of model over-parameterisation used by other studies, so included here for reference. The model considered to be optimal (i.e., high R_t^2, but without an integer loss of *YIC* compared to lower order models) is highlighted in bold and underlined.

Table 5 | Model structure, efficiency, measures of model parsimony and dynamic response characteristics for optimal CT-TF models for rainfall–streamflow for the periods 19 December 2012 to 3 January 2013 and 5 to 18 February 2013 of basins LI3, LI6, LI7 and LI8 at Llyn Brianne

	LI3		LI6		LI7		LI8	
Site	**19/12/12–3/1/13**	**5/2/13–18/2/13**	**19/12/12–3/1/13**	**5/2/13–18/2/13**	**19/12/12–3/1/13**	**5/2/13–18/2/13**	**19/12/12–3/1/13**	**5/2/13–18/2/13**
Model	[2 2 1]	[2 2 2]	[2 2 1]	[2 2 0]	[2 2 0]	[2 2 0]	[2 2 0]	[2 2 2]
R_t^2	0.93	0.89	0.93	0.85	0.92	0.85	0.90	0.87
YIC	− 6.67	− 6.55	− 7.28	− 7.28	− 7.07	− 5.81	− 6.46	-6.23
BIC	− 9,796.80	− 9,883.52	− 3,444.92	− 9,077.31	− 9,440.34	− 9,102.73	− 9,904.47	− 10,550.27
$S2 \times 100$	0.09	0.04	82.46	0.08	0.11	0.08	0.08	0.02
$condP \times 10$	9.28	8.94	9.33	8.52	9.20	8.49	8.96	8.71
TC fast component (hrs)	5.53	5.13	2.40	3.75	3.33	4.82	3.67	3.54
TC slow component (hrs)	33.43	58.97	24.54	53.20	36.40	64.65	34.66	64.98
fast%	55.39	75.09	55.25	63.85	56.88	68.22	70.46	83.60
slow%	44.61	24.91	44.75	36.15	43.12	31.78	29.54	16.40
SD of fast *TC* (hrs)	0.07	0.04	0.16	0.04	0.03	0.05	0.02	0.02
SD of slow *TC* (hrs)	1.1	6.6	110	5.8	2.4	8.5	2.5	5.3

Model structure is given as [Denominators, Numerators, Pure Time Delays]. The fast% term is percentage of response following a fast pathway of a second-order model (see Equation (9)), while the term SD of fast *TC* is the standard deviation of the fast *TC* from 1,000 Monte Carlo realisations. The steady state gain (SSG) is not presented as the rainfall time series used is an arithmetic average of the 15-minute totals for LI3 and LI6 rain gauges, rather than catchment-average totals per 15-minute intervals.

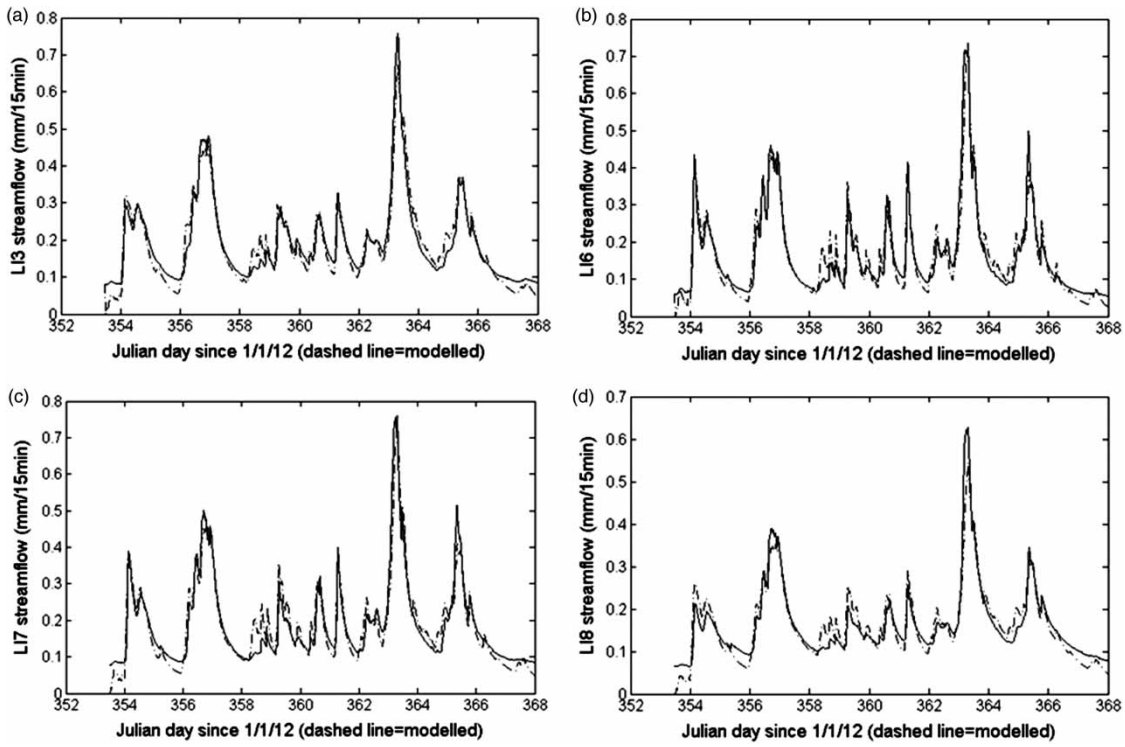

Figure 2 | Simulated streamflow (dashed line) from rainfall input together with observed streamflow (solid line) for (a) LI3, (b) LI6, (c) LI7 and (d) LI8 for the period 19 December 2012 to 3 January 2013.

a parallel decomposition has been shown to have a hydrological interpretation (e.g., Ockenden & Chappell 2011) whereas other forms of decomposition (e.g., feedback systems) lack a feasible hydrological interpretation. This parallel model comprises two *TC*s and the proportion of response associated with each *TC* (Table 5). The uncertainties in the *TC*s (expressed as standard deviations derived by Monte Carlo analysis) are also presented in Table 5. For the LI3 results, the frequency distributions of the fast and slow *TC*s are shown in Figure 3 as an illustration. A narrow range of uncertainty for both the slow and fast *TC*s was observed from this Monte Carlo analysis, with the exception of the slow response component for LI6 (Table 5).

A mechanistic hydrological interpretation of the identified *TC*s can be achieved with reference to such values derived by similar modelling approaches previously applied to a range of sites each with different streamflow generation mechanisms (Table 6). The time series of the simulated fast component for each of the four basins is shown in Figure 4(a) and the slow component in Figure 4(b).

The *TC*s for the fast component for the four experimental basins at Llyn Brianne ranged from 2.40 to 5.53 hours (Table 5). These values are, for example, much longer than those of measured overland flow on a tropical hillslope at 5 min or 0.08 hours (Chappell *et al*. 2006), but comparable to the response of a hillslope system elsewhere in the Cambrian mountains (i.e., 2.9 hours: Table 6) that has independent evidence of a dominance of shallow subsurface pathways in the soil (Chappell *et al*. 1990).

The *TC*s for the slow component of the four experimental basins during the 16-day winter (i.e., wet) period at Llyn Brianne ranged from 24.54 to 36.40 hours (Table 5). This range in *TC*s is a factor of 71 to 105 faster than that for a rainfall–streamflow response dominated by a single deep

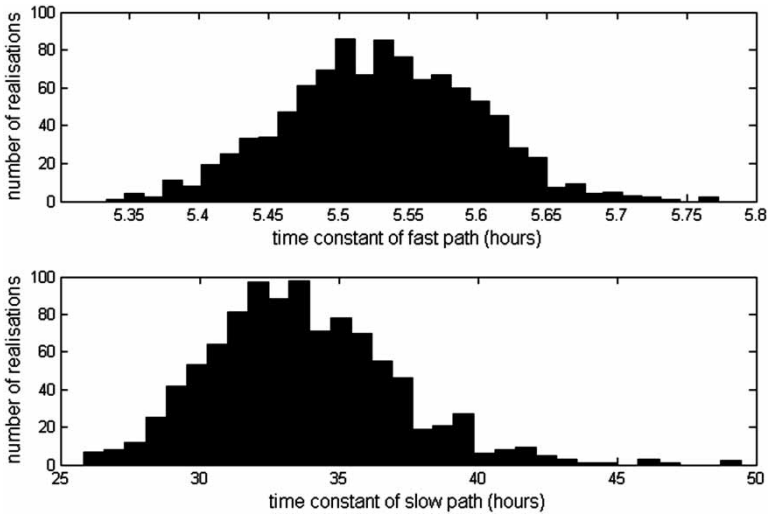

Figure 3 | Number of realisations of values of the fast response pathway (upper figure) and slow pathway (lower figure) derived from 1,000 Monte Carlo realisations of the decomposed [2 2 1] CT-TF model for rainfall–streamflow at LI3, for the period 19 December 2012 to 3 January 2013.

Table 6 | Selected *TC* of CT models (identified by RIVCBJID) re-applied to rainfall–streamflow time series from hillslopes and catchments within previous studies

TC	Dominant runoff process associated	Reference
5 min	Overland flow (infiltration excess primarily)	Chappell *et al*. (2006)
2.9 hours	Shallow subsurface flow from a hillside	Chappell *et al*. (1990)
100 hours	Fracture flow in Dartmouth slate	Chappell & Franks (1996); Birkinshaw & Webb (2010)
107 days	Deep pathway through a chalk aquifer	Ockenden & Chappell (2011)

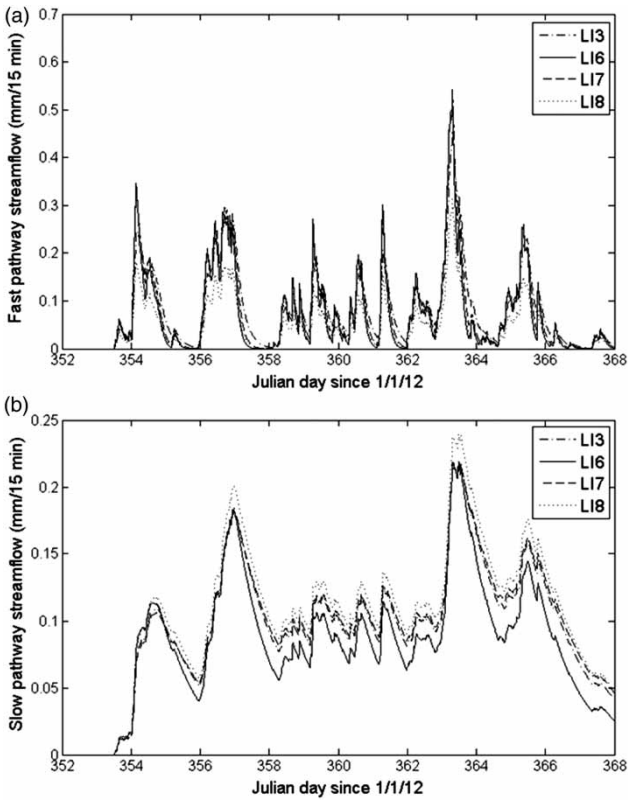

Figure 4 | Simulated streamflow for LI3, LI6, LI7 and LI8, where (a) shows the fast components of streamflow and (b) the slow components of streamflow (observable in the winter streamflow).

pathway through a chalk aquifer of 107 days or 2,568 hours (Ockenden & Chappell 2011). The range for the Brianne micro-basins in the winter is also a factor of 2.4 to 4.1 faster than that of a single pathway via fractures in Devonian slates at Slapton, UK (Table 6). However, this 4.2 day (100.8 hour) *TC* for Slapton is comparable to the slow component of flow derived from responses in the late summer, at a basin 7 km northwest of the four study basins (Jakeman *et al.* 1990). This finding may imply that an even slower component of response within LI3, LI6, LI7 and LI8 is not observable during the studied winter period because of the high antecedent moisture conditions. When the modelling approach is applied to the drier summer period, slower components derived from rock fractures (known to be present in LI6 and LI7: BGS 2005) may be identifiable. Fractures within the Lower Palaeozoic rocks elsewhere in the Cambrian Mountains are known to be active hydrologically (Shand *et al.* 2005). Furthermore, where a fault crosses the main stream within LI6 (Nant Esgair Garn) at 52° 07′ 57.74″ N 3° 43′ 13.36″ W, seepage with a high EC and high iron content has been measured (unpublished data). The presence of the 1–1.5 day (24–36 hour) slow component (Table 5) may, therefore, imply that a significant component of the response in the LI3, LI6, LI7 and LI8 streams during the winter months is sourced by a pathway with *TC*s intermediate between those of the soil horizons (cf. Chappell *et al.* 1990) and rock fractures. The lower slopes of LI6, LI7 and LI8 are known to have a layer of glacial till between the soil profile and the Lower Palaeozoic rocks (BGS 2005) that may be responsible for this 1–1.5 day (24–36 hour) response component. Glacial till is likely to be present at LI3 but not mapped because of a lack of exposures. The depth of till within the basins is currently unmeasured. The relative similarity of the *TC*s for the slower components of the four basins may imply a similar spatial extent and depth of glacial till, combined with the similar underlying geological formation (Reynolds & Norris 1990; BGS 2005) and relatively similar basin sizes (Table 2).

It is not clear how the varying proportions of different soil types (Table 2) have affected the *TC*s of the fast component; however, the apparent lack of the Histosol soils within LI3 (with their known flashy behaviour in the UK uplands: Gilman & Newson 1980; Holden & Burt 2003 Figure 3), may be responsible for its longer *TC* (Table 5). Basins LI3 and LI8 both have extensive forestry drainage and forest cover (of different extents), but do not have systematically different rainfall–streamflow responses (i.e., *TC*s) to the upland grasslands of LI6 and LI7. Consequently, the presence of forestry drainage and/or forest cover does not seem to have a significant impact on streamflow response in the Llyn Brianne basins.

To determine the transferability of the second-order linear models of rainfall–streamflow to a later winter period that also has H^+ data, the RIVCBJID algorithm was applied independently to a series of three storms that occurred between 5 and 18 February 2013. Again, a range of models with first- to fourth-order structures were identified with a pure time delay between zero and six time-steps. The optimal models and associated parameters for the four catchments are shown in Table 5 alongside the results for the earlier period. For this February period, purely linear second-order models [2 2 τ] were again identified as the optimal models and produced R_t^2 efficiency values in excess of 85%

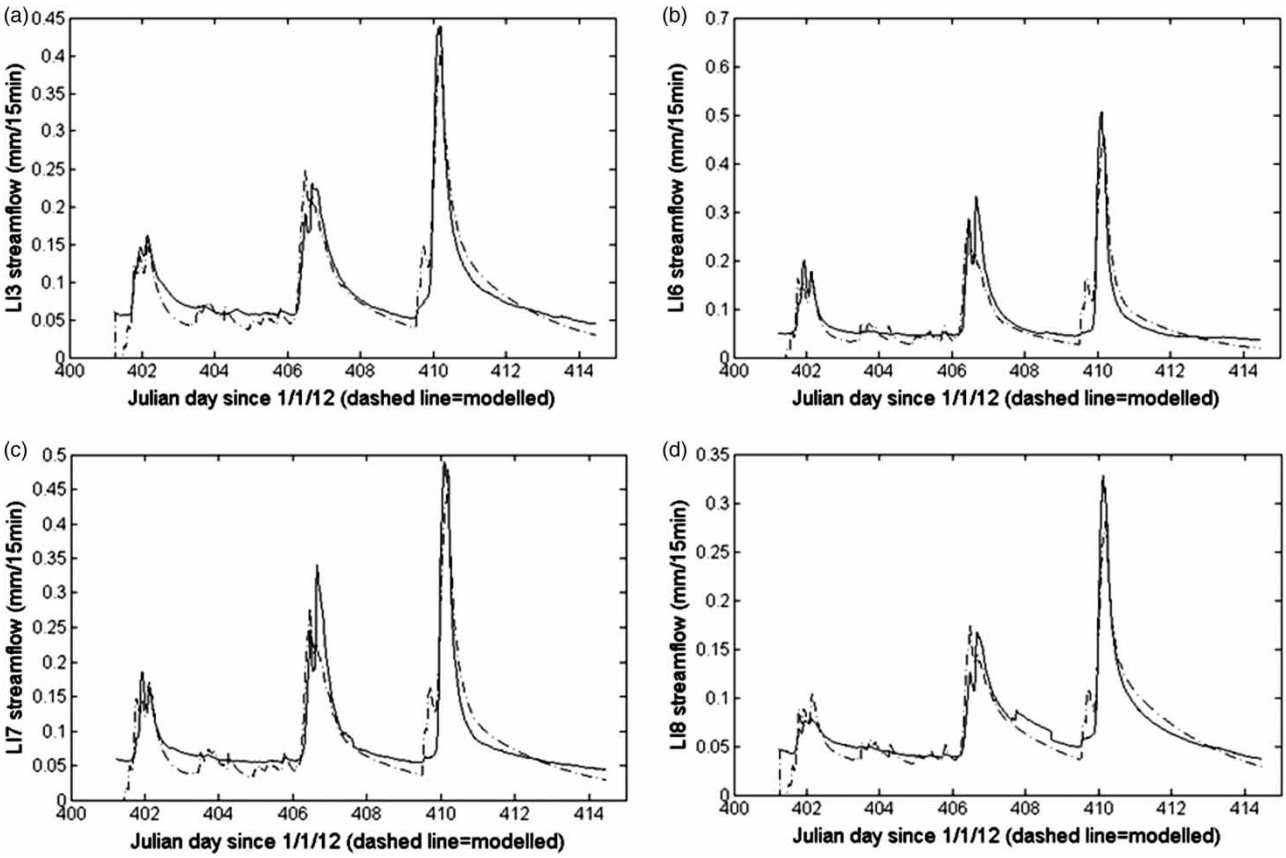

Figure 5 | Simulated streamflow (dashed line) from rainfall input together with observed streamflow (solid line) for (a) LI3, (b) LI6, (c) LI7 and (d) LI8, for the period 5 to 18 February 2013.

(Table 5; Figure 5). This provides *conditional validation* (Young 2001) that rainfall–streamflow response at Llyn Brianne during the winter consistently has a second-order model structure. For this second period the *TC* for the slow component doubled, however, this was offset by a significant reduction in the proportion of the response along the slow pathway (Table 5). The differences in the pure time delays between the two periods are very small, changing by zero to only two time-steps. Furthermore, there is no systematic shift in the fast *TC* between the two periods (Table 5).

Streamflow to H^+ concentration modelling

Given that a streamflow time series is an expression of the emergent behaviour of often complex and poorly defined hydrological pathways that carry solute responses (see, e.g., McDonnell *et al.* 2007), the next stage of analysis examined whether short-term dynamics in the H^+ concentration were associated with these streamflow dynamics (Objective 2). This stage involved quantifying the dynamic relationships between streamflow (mm per 15 min) and H^+ concentration (μeq/L per 15-min period) during a contiguous period of winter storms in February 2013. If a strong dynamic relationship is seen between the H^+ concentration and the streamflow it might be inferred that the processes leading to changes in the H^+ concentration through winter storms at Llyn Brianne are strongly hydrologically mediated.

Purely linear first-order CT-TF models, the simplest form of a dynamic model that may be presented, were able to identify between 82 and 97% of the variance in the H^+ concentration for the four streams (Table 7, Figure 6). For linear second-order models, the explanation ranged from 93 to 99% (Table 8; Figure 7). The improvement in model efficiency was most marked with LI3 where it increased from 82 to 93%. Furthermore, for LI3 the second-order structure better captured the later recessions (Figure 7), and had a

Table 7 | Model structure, efficiency, measures of model parsimony and dynamic response characteristics for optimal first-order CT-TF models for streamflow to H^+ concentration for the period 5 to 18 February 2013 for each catchment

Site	LI3	LI6	LI7	LI8
Model	[1 1 2]	[1 1 0]	[1 1 0]	[1 1 0]
R_t^2	0.82	0.97	0.96	0.84
YIC	− 1.73	− 10.80	− 9.48	− 8.01
BIC	6,189.13	− 1,860.66	− 3,184.75	10,738.66
$S2 \times 100$	1,283.00	22.82	8.04	468,000.00
$condP \times 10$	8.15	9.68	9.60	8.40
TC (hrs)	0.07	1.39	0.94	3.05

more negative *YIC* than the first-order model, indicating that this structure was most appropriate for these dynamics. By contrast, increasing model complexity to second-order models only improved simulation efficiency by 3, 2 and 0% for LI8, LI6 and LI7, respectively. This combined with the change in *YIC* of between +1.4 to +4.6 (Tables 7 and 8) indicated that interpretation of second-order dynamics for these three sites may not be justified. Given this, the DRCs from only first-order models for all four sites (including LI3 which is better described by a second-order model) are interpreted further, although the DRCs for all models are shown within Tables 7 and 8.

The *TC*s for the first-order relationship between H^+ concentration and the controlling streamflow range between 0.066 and 1.39 hours (or 3.9 and 83.6 min) for LI3, LI6 and LI7, while LI8 had a *TC* of 3.05 hours (or 183.3 min: Table 7). The variability between the four streams in their H^+ concentration response to streamflow (Table 7) is considerably larger than that between rainfall and the fast component of streamflow (Table 5); the coefficient of variation in the *TC*s of the former is 18% and the latter 91% (derived from data in Tables 5 and 7). This greater variability

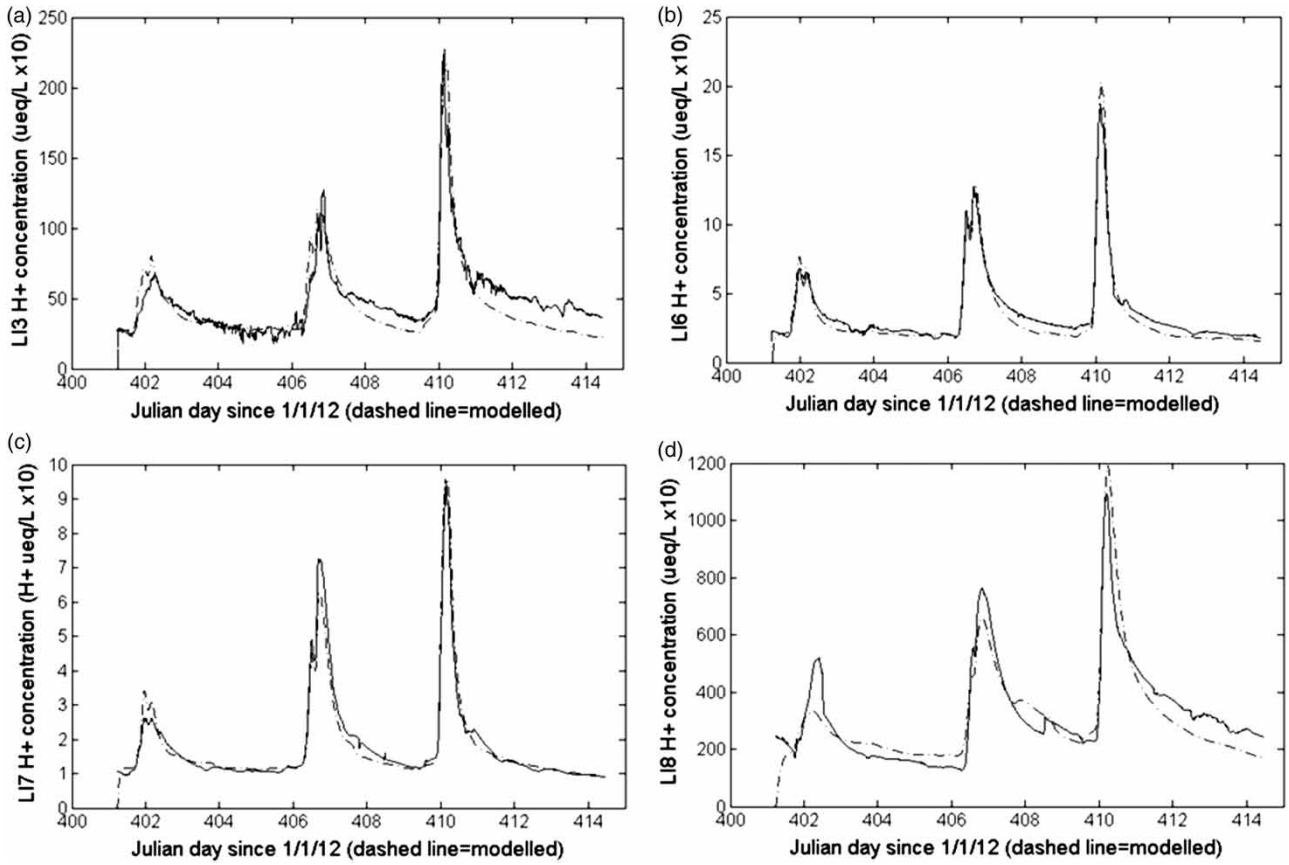

Figure 6 | First-order CT-TF simulated H^+ concentration (dashed line) from streamflow input together with observed H^+ concentration (solid line) for (a) LI3, (b) LI6, (c) LI7 and (d) LI8 for the period 5 to 18 February 2013.

Table 8 | Model structure, efficiency, measures of model parsimony and dynamic response characteristics of optimal second-order CT-TF models of streamflow to H^+ concentration for the period 5 to 18 February 2013 in each catchment

Site	LI3	LI6	LI7	LI8
Model	[2 2 1]	[2 2 1]	[2 2 0]	[2 2 1]
R_t^2	0.93	0.99	0.96	0.87
YIC	− 3.69	− 9.37	− 6.07	− 3.43
BIC	5,004.18	− 3,112.77	− 3,288.76	10,536.14
S2 ×*100*	5,016.00	8.37	7.32	392,300.00
condP ×*10*	9.28	9.88	9.36	8.66
TC fast component (hrs)	0.15	0.74	0.73	2.13
TC slow component (hrs)	273.64	32.13	11.40	490.79
fast%	46.21	22.60	11.25	40.92
slow%	53.79	77.40	88.75	59.08
SD of fast *TC* (hrs)	0.03	0.01	0.00	0.25
SD of slow *TC* (hrs)	900	0.12	0.07	11,000

will have resulted from a combination of the greater noise within the H^+ concentration compared to streamflow time series and due to short-term variations in the processes delivering hydrogen ions to the Llyn Brianne streams (Robson *et al.* 1993; Soulsby 1995). The longer *TC* for the H^+ response at LI8 is produced by the slower rise in H^+ concentration and the smaller relative range in H^+ concentration, i.e., a more damped response within the time series normalised by mean H^+ concentration; both of which are visible within Figure 8. The different response at LI8 may relate to the recent disturbance of 5 ha of acidic Histosol in its headwaters, delivering acid runoff later to the downstream point in the catchment than at the other sites. This tentative hypothesis requires additional experimental work along the Trawsnant stream.

When summer 2013 data are available and CT-TF models are applied to these data, it is expected that the *TC*s describing the relationship between streamflow and H^+ concentration will change. For example, the greater temperatures during the summer period may alter the mechanisms for release of H^+ ions (Nimick *et al.* 2011), and thereby alter the *TC*-related parameters in the models.

Over longer time periods other dynamic land-use related factors are likely to affect the relationship between streamflow and H^+ concentration (Neal *et al.* 1992; Ormerod & Durance 2009; Vanguelova *et al.* 2010). Use of the same purely linear first-order models with data from a winter period in 1986 (specifically 16 to 22 January 1986), studied by Littlewood (1989), may reflect these land-use change (LUC) differences. The model of streamflow to H^+ concentration for LI3 during this earlier period could be simulated to a high efficiency ($R_t^2 = 0.95$; Figure 9), but a longer *TC* of 2.3 hours was observed. This earlier period within LI3 had a complete forest cover of about 30-year-old conifers and it is interesting to note that the *TC* for this period is closer to that of the February 2013 monitoring period in the LI8 catchment (Table 5) which has over 95% forest cover of about 40-year-old conifers.

Streamflow to H^+ load modelling

The DBM modelling of the rainfall to streamflow relationship indicated that the response could be described by two components with quite distinct responses (i.e., *TC*s). Given that the H^+ concentration appears to be closely associated with the hydrological dynamics in the streamflow time series at Llyn Brianne (e.g., Figure 6), the investigation next addressed whether the export of H^+ (i.e., load) was associated with the two distinct response pathways identified for the streamflow generation. The final stage in this modelling was the identification of the relationship between rainfall and H^+ load, and how many separate components the time series of H^+ load may be divided into. If the load model has the same model structure as inferred for the streamflow response to rainfall then this

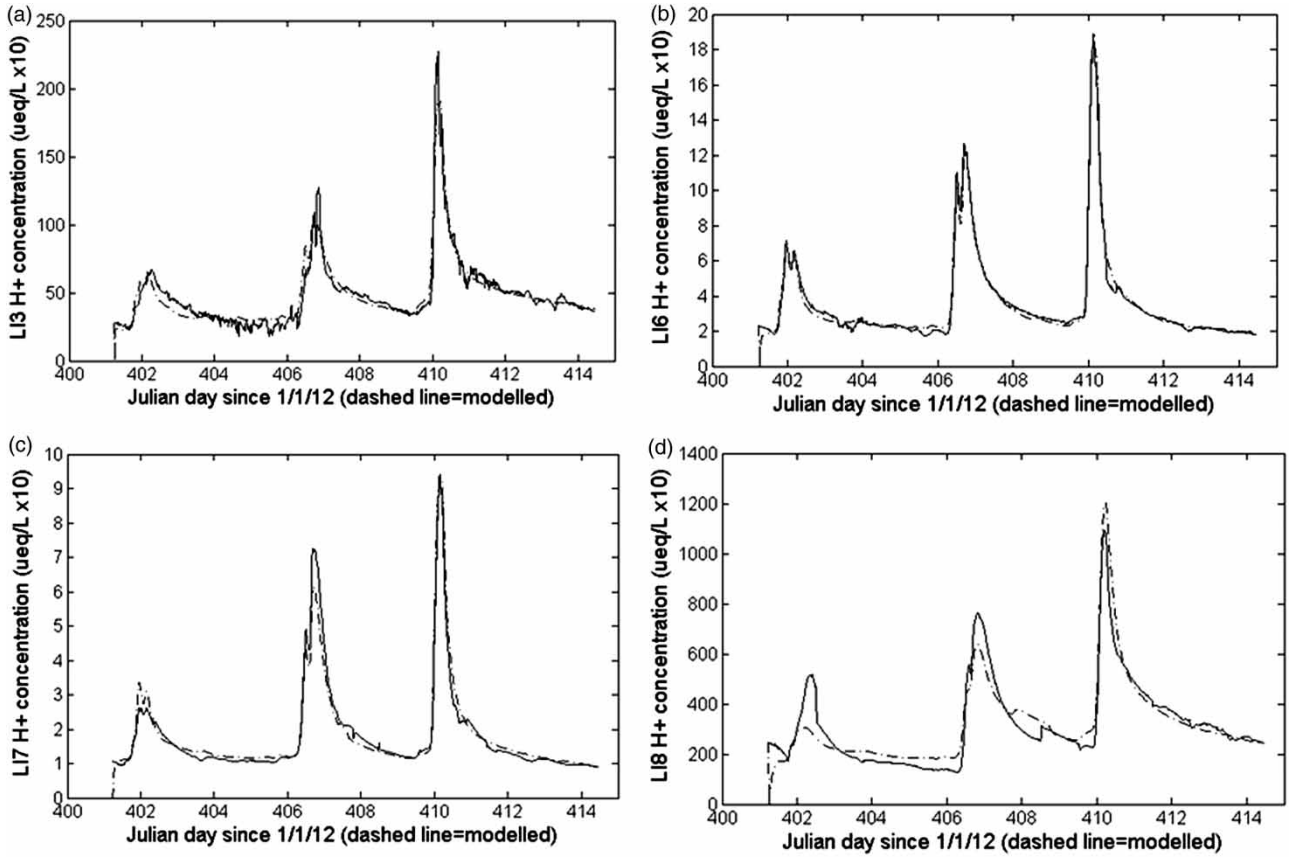

Figure 7 | Second-order CT-TF simulated H^+ concentration (dashed line) from streamflow input together with observed H^+ concentration (solid line) for (a) LI3, (b) LI6, (c) LI7 and (d) LI8 for the period 5 to 18 February 2013.

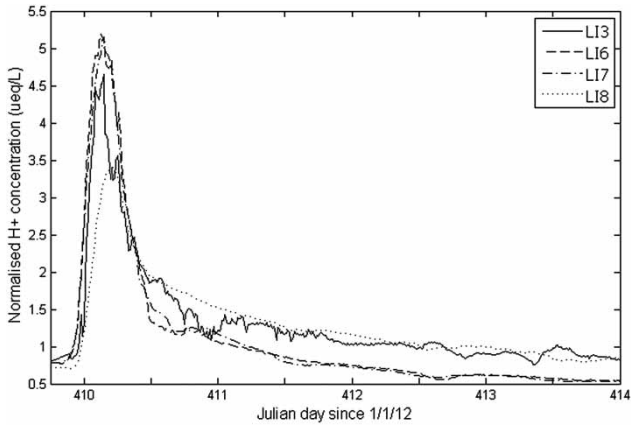

Figure 8 | Normalised observed H^+ concentration for all four streams during a single storm hydrograph over the period 14 to 18 February.

allows comparison of the characteristics of the two components of the response with those of the streamflow generation pathways (i.e., the *TC* and the portion of response along each pathway).

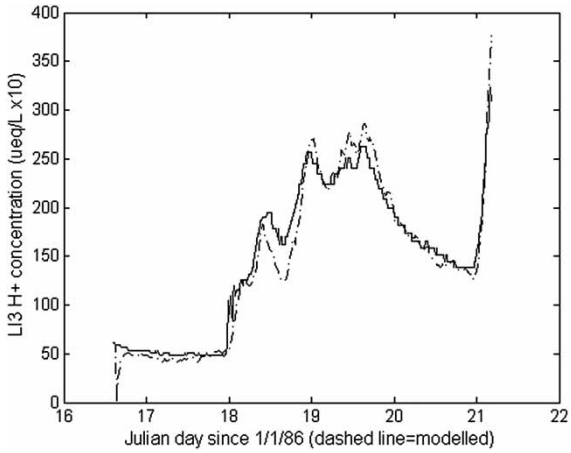

Figure 9 | First-order CT-TF simulated H^+ concentration (dashed line) from streamflow input together with observed H^+ concentration (solid line) for LI3, for the period 16 to 21 February 1986. The observed H^+ concentration and streamflow were previously analysed in Littlewood (1989) and obtained from the Environmental Information Data Centre of the Natural Environment Research Council (Licence: Llyn Brianne 22062012).

As with the rainfall–streamflow modelling a range of model structures from first- to sixth-order were investigated. As with the hydrological model, purely linear second-order models were optimal for all four sites (Table 9; Figure 10). This time series of H^+ load could then be readily decomposed into

Table 9 | Model structure, efficiency, measures of model parsimony and dynamic response characteristics of optimal CT-TF models for rainfall-H^+ load for the period 5 to 18 February 2013 in each catchment

Site	LI3	LI6	LI7	LI8
Model	[2 2 5]	[2 2 3]	[2 2 3]	[2 2 5]
R_t^2	0.71	0.75	0.73	0.75
YIC	− 3.60	− 2.78	− 2.39	− 1.64
BIC	14,527.02	8,824.92	6,750.25	20,125.46
S2 ×*100*	8,905,000	100,700	19,640	733,800,000
condP ×*10*	7.11	7.51	7.28	7.52
TC fast component (hrs)	2.50	2.29	3.42	7.49
TC slow component (hrs)	22.97	12.64	18.11	320.62
fast%	54.89	36.08	32.03	57.00
slow%	45.11	63.92	67.97	43.00
SD of fast *TC* (hrs)	0.12	0.26	0.46	0.34
SD of slow *TC* (hrs)	36	18	170	340
H^+ load per period (grams)	381.6	33.6	15.1	4,586.9

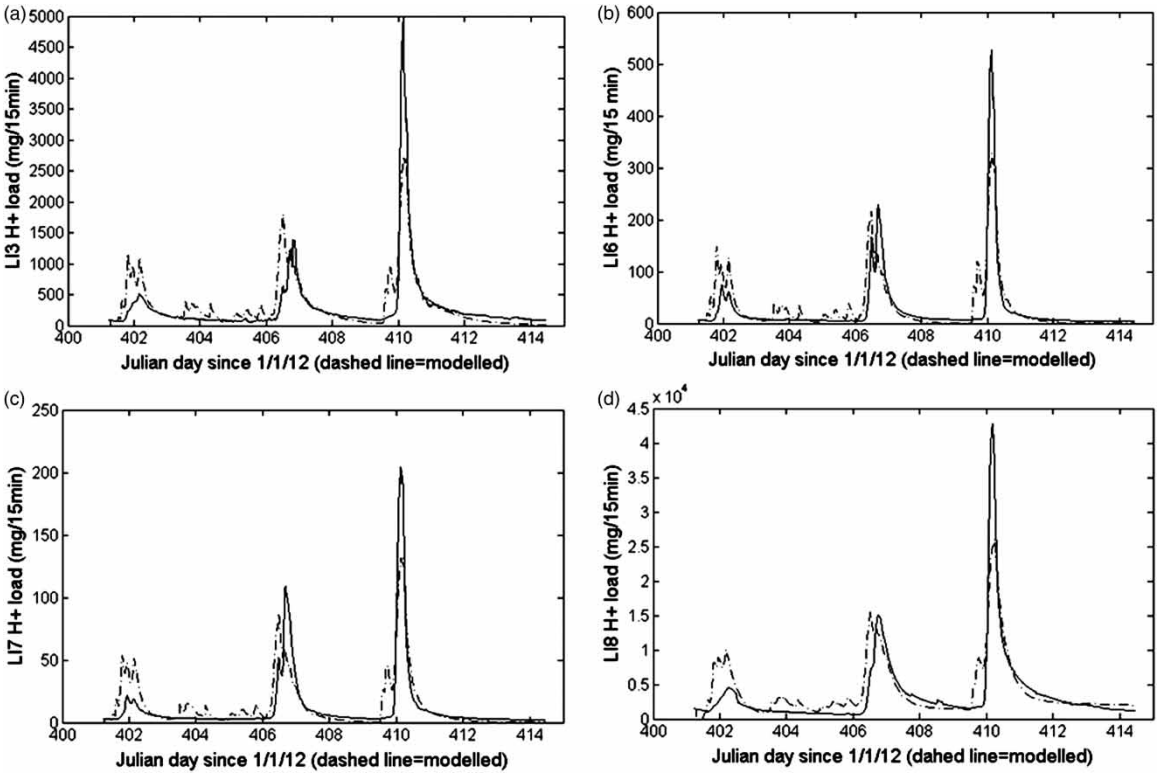

Figure 10 | Second-order CT-TF simulated H^+ load (dashed line) from rainfall input together with observed H^+ load (solid line) for (a) LI3, (b) LI6, (c) LI7 and (d) LI8, for the period 5 to 18 February 2013.

two components, as with the purely hydrological response.

The second-order models do explain two-thirds of the variance in the H^+ export (i.e., R_t^2 0.711 to 0.752) and are, therefore, models amenable to physical interpretation. The reduction in efficiency of modelling H^+ export rather than streamflow from rainfall was to be expected given the noise observable within the H^+ records, and the storm to storm variability in the H^+ behaviour observed previously at Llyn Brianne (Robson *et al.* 1993; Soulsby 1995). Some of this storm to storm variability will arise from variations in the ambient temperature of the system (Nimick *et al.* 2011), while some of the variability will relate to the interaction between H^+ and other dissolved solutes such as aluminium or HCO_3^- in the Llyn Brianne catchments (Neal & Christophersen 1989; Robson & Neal 1990; Robson *et al.* 1993).

The *TC*s for the fast response pathway are consistently faster for the H^+ export in LI3, LI6 and LI7 than those for the fast component of streamflow for the same February 2013 period (Tables 5 and 9; Figures 11–14). On average,

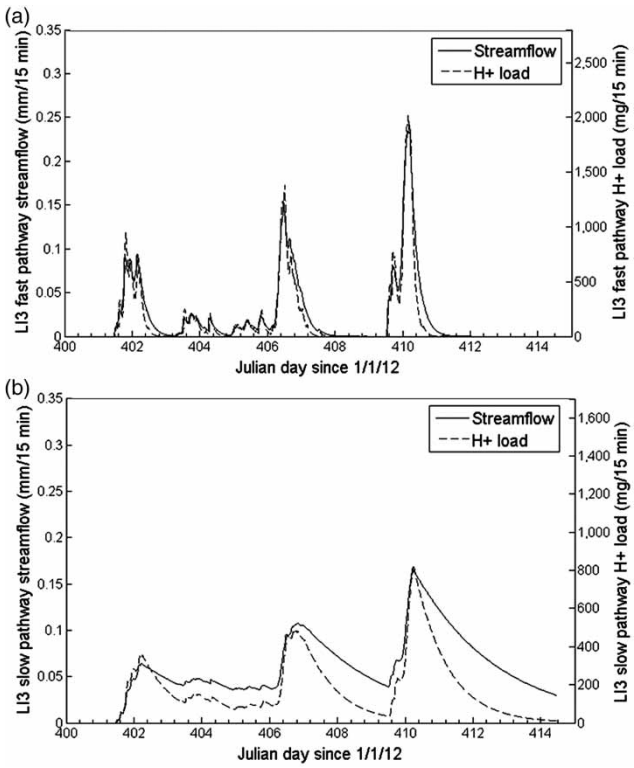

Figure 11 | CT-TF simulated (a) fast response pathway and (b) slow response pathway for LI3 streamflow and H^+ load from rainfall.

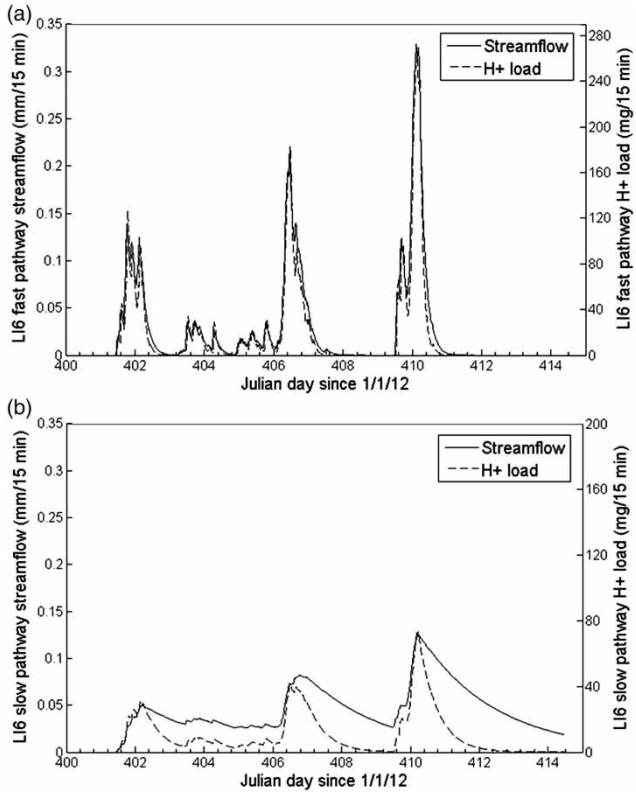

Figure 12 | CT-TF simulated (a) fast response pathway and (b) slow response pathway for LI6 streamflow and H^+ load from rainfall.

the fast H^+ export component in these three basins was 110 min faster than that for the fast water path (Tables 5 and 9). This indicates that a greater part of the hydrogen export is delivered in the earlier stages of the water flow response, indicating a positive hysteretic relationship between water flow and H^+ export, as also seen by Hooper *et al.* (1990). Hysteresis in the discharge–H^+ load relationship is also observed within raw observations, and underlines the importance of high-frequency sampling to capture these differences between the H^+ response on the rising versus falling stages of stream hydrographs. Where this hysteresis is present, this means that simple relationships with no dynamic storage effects between streamflow and H^+ export would be highly uncertain and should be avoided for estimation of long-term loads (Littlewood 1995).

The *TC* of the fast component of H^+ export for LI3, LI6 and LI7 is similar at 2.5, 2.3 and 3.4 hours, respectively; however, the export from LI8 has a *TC* of 7.5 hours (Table 9). As with the observation of the H^+ concentration

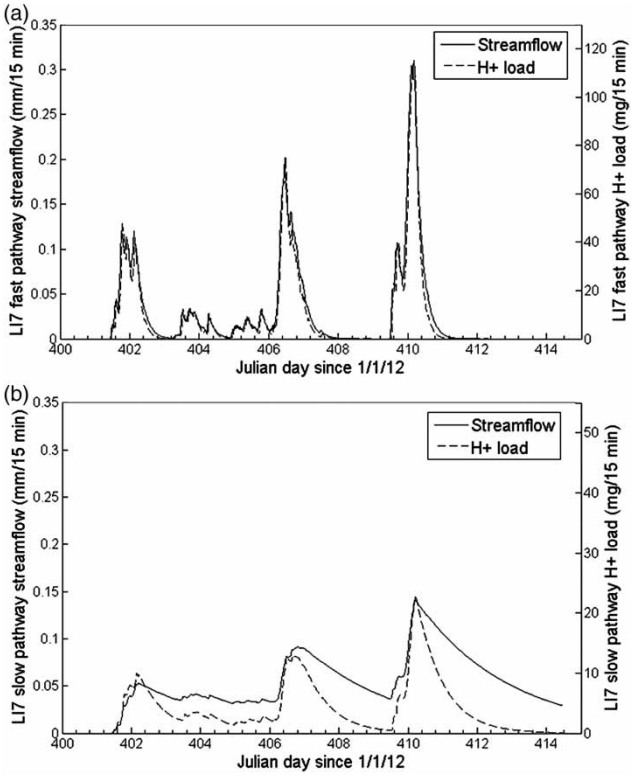

Figure 13 | CT-TF simulated (a) fast response pathway and (b) slow response pathway for LI7 streamflow and H^+ load from rainfall.

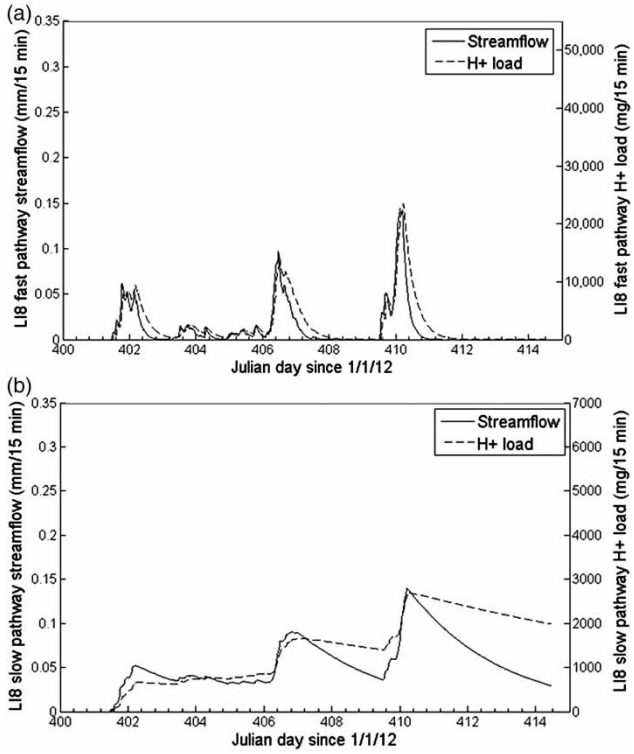

Figure 14 | CT-TF simulated (a) fast response pathway and (b) slow response pathway for LI8 streamflow and H^+ load from rainfall.

for this basin (Figure 8), the increase in the *TC* would appear to be caused by the slower rise in pH during the initial phase of the storm, and the generally more damped nature of the response relative to the background (Figure 15).

As with the fast component of the H^+ export, the *TC* of the slower component for LI3, LI6 and LI7 is considerably faster than the slower component of the water flow (Tables 5 and 9). For these basins, it is an average of 41 hours faster than the slower component of the water flow response. Again, this indicates that the H^+ is delivered in the earlier stages of the event, which implies that for both components of the response 'exhaustion effects' are present within the H^+ response. This may be explained by the H^+ ion being flushed from the catchment system and replaced with less hydrogen-rich waters as the event progresses. This may indicate the greater presence of newer water (i.e., a 'rainfall end-member') within the stream towards the latter stages of each rain storm (Hodgson & Evans 1997). Ion exchange may be an additional or alternative process driving the observed dynamics. The H^+

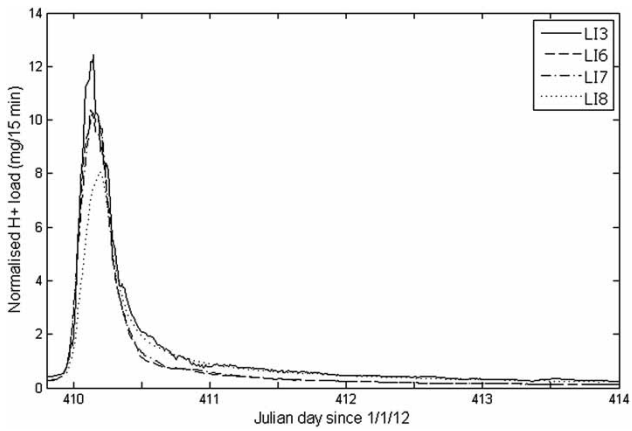

Figure 15 | Normalised observed H^+ load for all four streams during a storm hydrograph, 14 to 18 February 2013.

concentrations in between these events are relatively high (Figure 6). Considerably lower concentrations of H^+ have been recorded within these basins during the summer months and attributed to a component of water moving via a calcite-rich deeper pathway (Robson & Neal 1990),

perhaps through fractures within the underlying Lower Palaeozoic geology. Future modelling of the H^+ signals within the summer months is likely to identify a third, more damped pathway that is associated with the deeper components that only become identifiable during summer low flow. The working hypothesis is that the fast component of H^+ export is associated with flow through the soil (topsoil and subsoil) while the slower component of H^+ export during these winter months is associated with a deeper flow through the underlying glacial till, with a third component of flow through the rock fractures being unidentifiable in the winter period streamflow or H^+ records using RIVCBJID identification routines. Further direct investigations of the chemistry of these three components are needed to corroborate such a hypothesis, given that: (i) other hydrological pathways (e.g., soil pipes are observed in the basins), and (ii) dynamic biogeochemistry along unknown flow pathways (Chapman *et al.* 1993) may be responsible for the observed multiple components that are identifiable within the records of stream chemistry.

Total masses of H^+ exported were very different between the grassland and forest basins (Table 9); however, the *TC*s for the H^+ load were very similar for both the grassland and forest basins, indicating the importance of the basin hydrology over the impact of vegetation on biogeochemical dynamics.

Minimum monitoring interval

The Nyquist–Shannon sampling theorem indicates that monitoring or sampling must be at least twice that of the fastest *TC*, and in practice, at least six times faster (Young 2010). Table 10 shows the minimum sampling interval based upon all fast *TC*s for the rainfall to H^+ load (from Table 9), and for reference the rainfall to streamflow (from Table 5). For H^+ load these minimum sampling intervals range from 23 to 75 min (0.38–1.25 hours) for the four streams at Brianne, and 35 to 51 min (0.59–0.86 hours) for the streamflow dynamics (Table 10). Additionally, visual comparison of the storm response of the H^+ concentration (Figure 7) and that of streamflow (Figure 5) shows that the H^+ concentration changes as rapidly as the streamflow during storms. Given that monitoring of both streamflow and H^+ concentration was undertaken at a 15 min interval in streams at Brianne, the preceding analysis indicates that this should be sufficient to characterise the fundamental dynamics of streamflow, H^+ concentration and load response.

Table 10 | Maximum time between monitored values (max interval) required to capture the dominant modes of rainfall to H^+ load response for the basins LI3, LI6, LI7 and LI8 near Llyn Brianne, and for reference those for rainfall to streamflow

	Rainfall to streamflow models			Rainfall to H^+ load models		
		Max interval			Max interval	
Basin	Fast *TC* Mins	Mins	Hours	Fast *TC* Mins	Mins	Hours
L13	307.8	51	0.86	150.0	25	0.42
L16	225.0	38	0.63	137.4	23	0.38
L17	289.6	48	0.80	205.2	34	0.57
L18	212.4	35	0.59	449.4	75	1.25

The time constants (*TC*) (of the fast component of second-order, linear CT transfer functions) from which the minimum sampling intensities were derived, are also given. A 15-minute (0.25 hour) monitoring rate was used for H^+ concentration, rainfall and streamflow (and hence H^+ load) in LI3, LI6, LI7 and LI8.

The chemical concentration or load response of a stream during a storm (e.g., Figure 7) can be called the storm chemograph. An estimate of the *TC* of the recession of such a storm chemograph can be gained by finding the time from the chemograph peak to 63% of the return to the pre-storm concentration or load, assuming an exponential recession from a linear store. Table 11 shows the

Table 11 | Approximate *TC*s estimated from 63% of the recession (from storm peak to return to pre-storm value) of concentration chemographs from selected catchment studies with sub-daily sampling or monitoring during storms

Estimated *TC* (hours)	Variable	Reference	Figure
2	DOC	Inamdar *et al.* (2011)	9
4	Al	Goenaga & Williams (1988)	3
4	pH	Goenaga & Williams (1988)	2b
4	P	Jordan *et al.* (2007)	2 and 4
5	DOC	Inamdar *et al.* (2006)	3
6	pH	Hodgson & Evans (1997)	5
7	DOC	Jeong *et al.* (2012)	5
8	DOC	Boyer *et al.* (2000)	12
12	pH	Bonjean *et al.* (2007)	9
30	DOC	Fellman *et al.* (2009)	4

These estimates assume an exponential recession from a linear store. The figure showing the chemograph within the cited reference is provided.

estimated *TC*s from ten chemographs from key studies utilising sub-daily water quality data. The water quality variables cover pH, aluminium, total phosphorus and DOC. Nine of the ten *TC*s are in the range 2 to 12 hours suggesting a minimum required sampling interval (Young 2010) of approximately 0.33 to 2 hours or 20 to 120 min (i.e. *TC*/6) to properly describe the within-storm dynamics of these variables in these particular studies. Littlewood & Croke (2013) have demonstrated that estimates of model parameters fitted to under-sampled observations (i.e., where sampling was at a rate slower than the minimum required sampling interval) will be shifted from the true values obtained by fitting the same models to sufficiently sampled observations. The studies cited in Table 11 all have sub-daily water sampling or *in situ* monitoring intervals that exceed the *TC* (though not all exceed *TC*/6). Most water quality studies, even those undertaken in experimental catchments, however, do not have continuous sub-daily sampling of chemical concentration (Jordan *et al.* 2007; Bowes *et al.* 2009) and may, therefore, not have data to support robust modelling of storm chemographs.

CONCLUSIONS

Eight novel conclusions have arisen from this work:

1. The hydrological control of dynamics in the constituent H^+ concentration was affirmed from the strength of the dynamic relationship with the hydrological measure of streamflow ($R_t^2 > 89\%$), i.e., the lumped measure of often complex soil-water pathways, and potentially H^+ pathways, within headwater catchments.
2. The H^+ load modelling indicated that two separate response components were present within the relationship (i.e., second-order dynamics). This clear bimodal behaviour was also present within the optimal rainfall to streamflow models, suggesting that H^+ load was strongly moderated by the effects of these two hydrological response pathways. These two response components were identified from the observations by application of two objective statistical criteria (R_t^2, *YIC*), rather than assuming *a priori* a certain model structure, as in most non-DBM modelling studies.
3. The minimum sampling interval identified by the transfer function modelling indicates that for simulation of H^+ load requires minimum sampling intervals of 23, 25, 34 and 75 min for the headwater basins LI6, LI3, LI7 and LI8, respectively. These rates are within the range estimated from a preliminary set of key studies with high frequency sampling of chemical concentration through storms. Most water quality data-sets, however, lack such data (even for individual storms), and so may be inappropriate for developing or evaluating models that can capture the hydrological controls on water quality dynamics.
4. Comparison of the identified *TC*s of the hydrological response characteristics with those identified within other basins having independent corroboration of water pathways, indicated that a soil-water pathway may be responsible for the fast pathways at the Llyn Brianne basins, while the slower path (during the wet winter conditions) may be associated with pathways in underlying drift strata. While other studies and many temperate sites have suggested the importance of these two pathways, they have not been previously identified by inter-comparison of DRCs derived for reference sites (Table 6). Independent evidence of these two pathways within the studied Brianne basins is, however, required to strengthen or correct these tentative conclusions. A new measurement programme has been initiated to obtain direct observations of the two pathways (rather than estimate from their resultant impact on the streamflow response).
5. The response characteristics of the slower pathway are the least certain given the short duration of the modelled record relative to the *TC* of the slower pathway. Simulation of longer records is required to constrain the uncertainty within this *TC*. Furthermore, longer-term simulation that also includes drier conditions may allow the identification of even slower components; perhaps via hydrologically active rock fractures known to play a role within the hydrochemistry elsewhere within the Lower Palaeozoic Cambrian Mountains.
6. Relative to the purely hydrological response, the response of the H^+ load was considerably faster, indicating very rapid mixing and/or ion exchange processes to an input of rainwater to these catchments. Both fast and slow components of the load response did, however, show

clockwise hysteresis relative to the hydrological response components indicating a supply-limited process or exhaustion of the H^+ ions along the inferred pathways with the progression of a storm. Again, these pathway-specific interpretations need to be evaluated further following the planned new programme of continuous monitoring of H^+ concentration at different depths (i.e., overland flow, soil-water, water in the glacial till and water in rock fractures).

7. The basin that is primarily covered by mature conifers (i.e. LI8) exhibited a more delayed H^+ response at the start of storms and during storm recessions. Explanation of this phenomenon needs to be and will be explored with the new continuous monitoring of H^+ concentration in basin soils and below.
8. Kirchner (2006, 2009) and McDonnell *et al.* (2007) have stated that advances in the understanding of water pathways responsible for stream hydrograph response and the dynamics in stream water quality, demands the synchronous monitoring and analysis of water quality and hydrological variables. This study has demonstrated the H^+ concentration in headwater streams is: (i) closely associated with the hydrological dynamics, (ii) changes as quickly as the streamflow response during storms, and (iii) is information rich. With sufficient temporal sampling of H^+ concentration and streamflow, combined with a method that can robustly extract information from time series (notably the RIVCBJID algorithm for identifying CT transfer functions), time series of H^+ load can provide tentative hypotheses regarding water pathways responsible for stream hydrograph response and the dynamics in stream water quality.

While more H^+ observations and modelling at Brianne are required to further develop understanding of solute pathways, successes with this first stage of DURESS modelling do indicate that identified models of H^+ dynamics may be sufficiently robust to aid in the development and evaluation of new models of DOC and nitrate using the same approaches.

ACKNOWLEDGEMENTS

The authors would like to thank Mr Roger Davies, Mr Geoff Jones, Natural Resources Wales and Scottish Woodland for access to the research basins, and Natural Resources Wales (formerly Environment Agency Wales) for permission to install the flumes and conduct dilution gauging. The assistance of Mr Goronwy Thomas, Dr James Heath, Mr David Norris, Dr Ben Surridge and Dr Wlodek Tych with installation of field instruments and Dr Gemma Davies for the derivation of basin areas is gratefully acknowledged. Dr Ian Littlewood and the Environmental Information Data Centre of the Natural Environment Research Council are thanked for access to the LI3 data from years 1986 and 1989 (Licence: Llyn Brianne 22062012). The authors gratefully acknowledge constructive comments on the manuscript from two anonymous reviewers and the Editor. The work is funded by Natural Environment Research Council grant NE/J014826/1.

REFERENCES

Beven, K. J. 2012 *Rainfall-runoff Modelling: The Primer*, 2nd edn. Wiley-Blackwell, Chichester, UK.

Beven, K. & Westerburg, I. 2011 On red herrings and real herrings: disinformation and information in hydrological inference. *Hydrol. Process.* **25**, 1676–1680.

Bieroza, M. & Heathwaite, L. 2012 In-stream nutrient dynamics observed by automated high frequency monitoring (River Leith, Cumbria, UK). Paper presented at BHS Eleventh National Symposium, Hydrology for a changing world. Dundee, UK, 09/07/11–11/07/12.

Bird, S. C., Walsh, R. P. D. & Littlewood, I. G. 1990 Catchment characteristics and basin hydrology: their effects on streamwater acidity. In: *Acid Waters in Wales* (R. W. Edwards, A. S. Gee & J. H. Stoner, eds). Kluwer, Dordrecht.

Birkel, C., Dunn, S. M., Tetzlaff, D. & Soulsby, C. 2010 Assessing the value of high-resolution isotope tracer data in the stepwise development of a lumped conceptual rainfall-runoff model. *Hydrol. Process.* **24**, 2335–2348.

Birkinshaw, S. J. & Webb, B. 2010 Flow pathways in the Slapton Wood catchment using temperature as a tracer. *J. Hydrol.* **383**, 269–279.

Bonjean, M. C., Hutchins, M. & Neal, C. 2007 Acid episodes in the Allt a' Mharcaidh, Scotland: an investigation based on sub-hourly monitoring data and climatic patterns. *Hydrol. Earth Syst. Sc.* **11**, 340–355.

Bowes, M. J., Smith, J. T. & Neal, C. 2009 The value of high-resolution nutrient monitoring: a case study of the River Frome, Dorset, UK. *J. Hydrol.* **378**, 82–96.

Box, G. E. P., Jenkins, G. M. & Reinsel, G. C. 2008 *Time Series Analysis: Forecasting and Control*, 4th edn. Wiley, Hoboken, NJ, USA.

Boyer, E. W., Hornberger, G. M., Bencala, K. E. & McKnight, D. M. 2000 Effects of asynchronous snowmelt on flushing of dissolved organic carbon: a mixing model approach. *Hydrol. Process.* **14**, 3291–3308.

British Geological Survey. 2005 *Builth Wells. England and Wales Sheet 196. Solid and Drift Geology. 1:50,000.* British Geological Survey, Keyworth, UK.

Chapman, P. J., Reynolds, B. & Wheater, H. S. 1993 Hydrochemical changes along stormflow pathways in a small moorland headwater catchment in Mid-Wales, UK. *J. Hydrol.* **151**, 241–266.

Chappell, N. A. & Franks, S. W. 1996 Property distributions and flow structure in the Slapton Wood Catchment. *Field Stud.* **8**, 559–575.

Chappell, N. A., Ternan, J. L., Williams, A. G. & Reynolds, B. 1990 Preliminary analysis of water and solute movement beneath a coniferous hillslope in mid-Wales, UK. *J. Hydrol.* **116**, 201–215.

Chappell, N. A., Tych, W., Chotai, A., Bidin, K., Sinun, W. & Chiew, T. H. 2006 BARUMODEL: combined data based mechanistic models of runoff response in a managed rainforest catchment. *Forest Ecol. Manag.* **224**, 58–80.

Chappell, N. A., Bonell, M., Barnes, C. J. & Tych, W. 2012 Tropical cyclone effects on rapid runoff responses: quantifying with new continuous-time transfer function models. In: *Revisiting Experimental Catchment Studies in Forest Hydrology* (A. A. Webb, M. Bonell, L. Bren, P. N. J. Lane, D. McGuire, D. G. Neary, J. Nettles, D. F. Scott, J. Stednik & Y. Wang, eds). IAHS Publication 353, IAHS Press, Wallingford, UK, pp. 82–93.

Christophersen, N., Seip, H. M. & Wright, R. F. 1982 A model for streamwater chemistry at Birkenes, Norway. *Water Resour. Res.* **18**, 977–996.

Christophersen, N., Neal, R. P., Vogt, R. D. & Andersen, S. 1990 Modelling streamwater chemistry as a mixture of soilwater end-members – a step towards second-generation acidification models. *J. Hydrol.* **116**, 307–320.

Christophersen, N., Neal, C. & Hooper, R. P. 1993 Modelling the hydrochemistry of catchments: a challenge for the scientific method. *J. Hydrol.* **152**, 1–12.

Cosby, B. J., Wright, R. F., Hornberger, G. M. & Galloway, J. N. 1985 Modeling the effects of acid deposition: estimation of long-term water quality responses in a small forested catchment. *Water Resour. Res.* **21**, 1591–1601.

Dunford, R. W., Donoghue, D. N. M. & Burt, T. P. 2012 Forest land cover continues to exacerbate freshwater acidification despite decline in sulphate emissions. *Environ. Pollut.* **167**, 58–69.

Evans, C. D., Jones, T. G., Burden, A., Ostle, N., Zielinski, P., Cooper, M. D. A., Peacock, M., Clark, J. M., Oulehle, F., Cooper, D. & Freeman, C. 2012 Acidity controls on dissolved organic carbon mobility in organic soils. *Glob. Change Biol.* **18**, 3317–3331.

FAO-Unesco 1990 *Soil Map of the World, Revised Legend*. FAO, Rome, Italy, 119 pp.

Fellman, J. B., Hood, E., Edwards, R. T. & D'Amore, D. V. 2009 Changes in the concentration, biodegradability, and fluorescent properties of dissolved organic matter during stormflows in coastal temperate watersheds. *J. Geophys. Res.* **114**.

Fitzhugh, R. D., Furman, T. & Cosby, B. J. 1999 Longitudinal and seasonal patterns of stream acidity in a headwater catchment on the Appalachian Plateau, West Virginia. *Biogeochemistry* **47**, 39–62.

Fowler, D., Cape, J. N. & Unsworth, M. H. 1989 Deposition of atmospheric pollution on forests. *Philos. T. Roy. Soc. B* **324**, 247–265.

Garnier, H., Young, P. C., Thil, S. & Gilson, M. 2008 Continuous-time data-based modelling of environmental systems. *Revue electronique e-STA (Sciences et Technologies pour l'Automatique)* **5**, 1–8.

Gilman, K. & Newson, M. D. 1980 *Soil Pipes and Pipeflow; A Hydrological Study in upland Wales*. British Geomorphological Research Group Research Monograph No. 1, Geo Books, Norwich, UK.

Goenaga, X. & Williams, D. J. A. 1988 Aluminium speciation in surface waters from a Welsh upland area. *Environ. Pollut.* **52**, 131–149.

Grande, J. A., Andújar, J. M., Aroba, J., de la Torre, M. L. & Beltrán, R. 2005 Precipitation, pH and metal load in AMD river basins: an application of fuzzy clustering algorithms to the process characterization. *J. Environ. Monitor.* **7**, 325–334.

Grip, H., Jansson, P.-E., Johnsson, H. & Nilsson, S. I. 1985 Application of the 'Birkenes' model to two forested catchments on the Swedish west coast. *Ecol. Bull.* **37**, 176–192.

Halliday, S. J., Wade, A. J., Skeffington, R. A., Neal, C., Reynolds, B., Rowland, P., Neal, M. & Norris, D. 2012 An analysis of long-term trends, seasonality and short-term dynamics in water quality data from Plynlimon, Wales. *Sci. Total. Environ.* **434**, 186–200.

Harmel, R. D., Cooper, R. J., Slade, R. M., Haney, R. L. & Arnold, J. G. 2006 Cumulative uncertainty in measured streamflow and water quality data for small watersheds. *Trans. ASABE* **49**, 689–701.

Hodgson, P. & Evans, J. G. 1997 Continuous pH, electrical conductivity and temperature measurement at Plynlimon: towards an integrated, reliable and low maintenance instrument system. *Hydrol. Earth Syst. Sci.* **1**, 653–660.

Holden, J. & Burt, T. B. 2003 Runoff production in blanket peat covered catchments. *Water Resour. Res.* **39**, 1191.

Hooper, R. P., Christophersen, N. & Peters, N. E. 1990 Modelling streamwater chemistry as a mixture of soilwater end-members – an application to the Panola Mountain catchment, Georgia, U.S.A. *J. Hydrol.* **116**, 321–343.

Inamdar, S. P., O'Leary, N., Mitchell, M. J. & Riley, J. T. 2006 The impact of storm events on solute exports from a glaciated forested watershed in western New York, USA. *Hydrol. Process.* **20**, 3423–3439.

Inamdar, S. P., Singh, S., Dutta, S., Levia, D., Mitchell, M., Scott, D., Bais, H. & McHale, P. 2011 Fluorescence characteristics and sources of dissolved organic matter for stream water

during storm events in a forested mid-Atlantic watershed. *J. Geophys. Res.* **116**.

Jakeman, A. J. & Hornberger, G. M. 1993 How much complexity is warranted in a rainfall-runoff model? *Water Resour. Res.* **29**, 2637–2649.

Jakeman, A. J., Littlewood, I. G. & Whitehead, P. G. 1990 Computation of the instantaneous unit hydrograph and identifiable component flows with application to two small upland catchments. *J. Hydrol.* **117**, 275–300.

Jeong, J.-J., Bartsch, S., Fleckenstein, J., Matzner, E., Tenhunen, J. D., Lee, S. D., Park, S. D. & Park, J.-H. 2012 Differential storm responses of dissolved and particulate organic carbon in a mountainous headstream, investigated by high-frequency in-situ optical measurements. *J. Geophys. Res* **117**, G03013.

Jordan, P., Arnscheidt, J., McGrogan, H. & McCormick, S. 2007 Characterising phosphorus transfers in rural catchments using a continuous bank-side analyser. *Hydrol. Earth Syst. Sci.* **11**, 372–381.

Kennard, M. J., Pusey, B. J., Olden, J. D., MacKay, S. J., Stein, J. L. & Marsh, N. 2010 Classification of natural flow regimes in Australia to support environmental flow management. *Freshwater Biol.* **55**, 171–193.

Kirchner, J. W. 2006 Getting the right answers for the right reasons: Linking measurements, analyses, and models to advance the science of hydrology. *Water Resour. Res.* **42**, W03S04.

Kirchner, J. W. 2009 Catchments as simple dynamical systems: catchment characterization, rainfall-runoff modelling, and doing hydrology backward. *Water Resour. Res.* **45**, W02429.

Kirchner, J. W. & Neal, C. 2013 Universal fractal scaling in stream chemistry and its implications for solute transport and water quality trend detection. *PNAS* **110**, 12213–12218.

Kirchner, J. W., Feng, X., Neal, C. & Robson, A. J. 2004 The fine structure of water-quality dynamics: the (high-frequency) wave of the future. *Hydrol. Process.* **18**, 1353–1359.

Langan, S. J. & Whitehead, P. G. 1987 The application of time-series modelling to short-term streamwater acidification in upland Scotland. *IAHS-AIHS Publication* **167**, 75–87.

Langan, S. J., Fransson, L. & Vanguelova, E. 2009 Dynamic modelling of the response of UK forest soils to changes in acid deposition using the SAFE model. *Sci. Total Environ.* **407**, 5605–5619.

Lepori, F., Barbieri, A. & Ormerod, S. J. 2003 Effects of episodic acidification on macroinvertebrate assemblages in Swiss Alpine streams. *Freshwater Biol.* **48**, 1873–1885.

Littlewood, L. G. 1989 The Dynamics of Acid Runoff from Moorland and Conifer Afforested Catchments Draining into Llyn Brianne, Wales. PhD Thesis, University of Wales.

Littlewood, I. G. 1995 Hydrological regimes, sampling strategies, and assessment of errors in mass load estimates for United Kingdom rivers. *Environ. Int.* **21**, 211–220.

Littlewood, I. G. 2003 Improved unit hydrograph identification for seven Welsh rivers: implications for estimating continuous streamflow at ungauged sites. *Hydrol. Sci. J.* **48**, 743–762.

Littlewood, I. G. & Croke, B. F. W. 2013 Effects of data time-step on the accuracy of calibrated rainfall–streamflow model parameters: practical aspects of uncertainty reduction. *Hydrol. Res.* **44**, 430–440.

Malcolm, I. A., Soulsby, C. & Youngson, A. F. 2006 High-frequency logging technologies reveal state-dependent hyporheic process dynamics: implications for hydroecological studies. *Hydrol. Process.* **20**, 615–622.

McDonnell, J. J., Sivapalan, M., Vaché, K., Dunn, S., Grant, G., Haggerty, R., Hinz, C., Hooper, R., Kirchner, J., Roderick, M. L., Selker, J. & Weiler, M. 2007 Moving beyond heterogeneity and process complexity: A new vision for watershed hydrology. *Water Resour. Res.* **43**, W07301.

Medici, C., Wade, A. J. & Francés, F. 2012 Does increased hydrochemical model complexity decrease robustness? *J. Hydrol.* **440**, 1–13.

Monteith, D. T., Hildrew, A. G., Flower, R. J., Raven, P. J., Beaumont, W. R. B., Collen, P., Kreiser, A. M., Shilland, E. M. & Winterbottom, J. H. 2005 Biological responses to the chemical recovery of acidified fresh waters in the UK. *Environ. Pollut.* **137**, 83–101.

Monteith, D. T., Stoddard, J. L., Evans, C., de Wit, H., Forsius, M., Hogasen, T., Wilander, A., Skelkvale, B. L., Jeffries, D. S., Vuorenmaa, J., Keller, B., Kopacek, J. & Vesely, J. 2007 Dissolved organic carbon trends resulting from changes in atmospheric deposition chemistry. *Nature* **450**, 537–541.

Neal, C. & Christophersen, N. 1989 Inorganic aluminium-hydrogen ion relationships for acidifed streams; the role of water mixing processes. *Sci. Total Environ.* **80**, 195–203.

Neal, C., Robson, A., Reynolds, B. & Jenkins, A. 1992 Prediction of future short term stream chemistry – A modelling approach. *J. Hydrol.* **130**, 87–103.

Neal, C., Reynolds, B., Rowland, P., Norris, D., Kirchner, J. W., Neal, M., Sleep, D., Lawlor, A., Woods, C., Thacker, S., Guyatt, H., Vincent, C., Hockenhull, K., Wickham, H., Harman, S. & Armstrong, L. 2012 High-frequency water quality time series in precipitation and streamflow: from fragmentary signals to scientific challenge. *Sci. Total Environ.* **434**, 3–12.

Nelson, C. E., Bennett, D. M. & Cardinale, B. J. 2013 Consistency and sensitivity of stream periphyton community structural and functional responses to nutrient enrichment. *Ecol. Appl.* **23**, 159–173.

Nimick, D. A., Gammons, C. H. & Parker, S. R. 2011 Diel biogeochemical processes and their effect on the aqueous chemistry of streams: a review. *Chem. Geol.* **283**, 3–17.

Ocampo, C. J., Oldham, C. E., Sivapalan, M. & Turner, J. V. 2006 Hydrological versus biogeochemical controls on catchment nitrate export: a test of the flushing mechanism. *Hydrol. Process.* **20**, 4269–4286.

Ockenden, M. C. & Chappell, N. A. 2011 Identification of the dominant runoff pathways from the data-based mechanistic modelling of nested catchments in temperate UK. *J. Hydrol.* **402**, 71–79.

Ockenden, M. C., Chappell, N. A. & Neal, C. 2013 Quantifying the differential contributions of deep groundwater to streamflow in nested basins, using both water quality characteristics and water balance. *Hydrol. Res.* in press.

Ormerod, S. J. & Durance, I. 2009 Restoration and recovery from acidification in upland Welsh streams over 25 years. *J. Appl. Ecol.* **46**, 164–174.

Potts, A. S. 1971 Fossil cryonival features in central Wales. *Geogr. Ann. A* **53**, 39–51.

Reynolds, B. & Norris, D. A. 1990 *Llyn Brianne Acid Waters Project – Summary of Catchment Characteristics*. Institute of Terrestrial Ecology, 45 pp.

Robson, A. & Neal, C. 1990 Hydrograph separation using chemical techniques: an application to catchments in mid-Wales. *J. Hydrol.* **116**, 345–363.

Robson, A., Neal, C., Hill, S. & Smith, C. J. 1993 Linking variations in short-term and medium-term stream chemistry to rainfall inputs – some observations at Plynlimon, mid-Wales. *J. Hydrol.* **114**, 291–310.

Shand, P., Abesser, C., Farr, G., Wilton, N., Lapworth, D. J., Gooddy, D. C., Haria, A. & Hargreaves, R. L. 2005 *T*he Ordovician and Silurian meta-sedimentary aquifers of central and south-west Wales. Baseline Report Series 17. Technical Report NC/99/74/17. Environment Agency National Groundwater & Contaminated Land Centre.

Shaw, E. M., Beven, K. J., Chappell, N. A. & Lamb, R. 2010 *Hydrology in Practice*, 4th edn. Taylor and Francis, Abingdon, UK.

Simon, K. S., Simon, M. A. & Benfield, E. F. 2009 Variation in ecosystem function in Appalachian streams along an acidity gradient. *Ecol. Appl.* **19**, 1147–1160.

Soulsby, C. 1995 Contrasts in storm event hydrochemistry in an acidic afforested catchment in upland Wales. *J. Hydrol.* **170**, 159–179.

Stoner, J. H., Gee, A. S. & Wade, K. R. 1984 The effects of acidification on the ecology of streams in the Upper Tywi catchment in West Wales. *Environ. Pollut. A* **25**, 125–157.

Taylor, C. J., Pedregal, D. J., Young, P. C. & Tych, W. 2007 Environmental time series analysis and forecasting with the CAPTAIN toolbox. *Environ. Modell. Softw.* **22**, 797–814.

Vanguelova, E. I., Benham, S., Pitman, R., Moffat, A. J., Broadmeadow, M., Nisbet, T., Durrant, D., Barsoum, N., Wilkinson, M., Bochereau, F., Hutchings, T., Broadmeadow, S., Crow, P., Taylor, P. & Durrant Houston, T. 2010 Chemical fluxes in time through forest ecosystems in the UK – Soil response to pollution recovery. *Environ. Pollut.* **158**, 1857–1869.

Weatherley, N. S. & Ormerod, S. J. 1987 The impact of acidification on macroinvertebrate assemblages in Welsh streams: towards an empirical model. *Environ. Pollut.* **46**, 223–240.

Weiler, M., McGlynn, B. L., McGuire, K. J. & McDonnell, J. J. 2003 How does rainfall become runoff? A combined tracer and runoff transfer function approach. *Water Resour. Res.* **39**, 1315.

Whitehead, P. G. & Crossman, J. 2012 Macronutrient cycles and climate change: key science areas and an international perspective. *Sci. Total Environ.* **434**, 13–17.

Whitehead, P. G., Bird, S., Hornung, M., Cosby, J., Neal, C. & Paricos, P. 1988 Stream acidification trends in the Welsh Uplands – a modelling study of the Llyn Brianne catchments. *J. Hydrol.* **101**, 191–212.

Yevenes, M. A. & Mannaerts, C. M. 2012 Untangling hydrological pathways and nitrate sources by chemical appraisal in a stream network of a reservoir catchment. *Hydrol. Earth Syst. Sci.* **16**, 787–799.

Young, P. C. 2001 Data-based mechanistic modelling and validation of rainfall-flow processes. In: *Model Validation: Perspectives in Hydrological Science* (M. G. Anderson & P. D. Bates, eds). J. Wiley, Chichester, UK, pp. 117–161.

Young, P. C. 2008 The refined instrumental variable method. *J. Eur. Syst. Automat.* **42**, 149–179.

Young, P. C. 2010 The estimation of continuous-time rainfall-flow models for flood risk management. In: *Role of Hydrology in Managing Consequences of a Changing Global Environment* (C. Walsh, ed.). British Hydrological Society, Newcastle University, Newcastle upon Tyne, pp. 303–310.

Young, P. C. 2013 Hypothetico-inductive data-based mechanistic modeling of hydrological systems. *Water Resour. Res.* **49**, 915–935.

Young, P. C. & Garnier, H. 2006 Identification and estimation of continuous-time, data-based mechanistic (DBM) models for environmental systems. *Environ. Modell. Softw.* **21**, 1055–1072.

First received 25 September 2013; accepted in revised form 10 March 2014. Available online 7 April 2014